Interannual Variability in the Northern Hemisphere Winter Middle Atmosphere in Control and Perturbed Experiments with the GFDL SKYHI General Circulation Model

KEVIN HAMILTON

Geophysical Fluid Dynamics Laboratory/NOAA, Princeton University, Princeton, New Jersey

(Manuscript received 2 December 1993, in final form 13 May 1994)

ABSTRACT

This paper reports on interannual variability of the Northern Hemisphere winter stratospheric circulation as simulated by the 40-level GFDL "SKYHI" general circulation model. A 31-year control simulation was performed using a climatological annual cycle of sea surface temperatures. The interannual variability of the stratospheric circulation in this model has some realistic features. In particular, the simulated variance of monthly mean, zonal-mean temperature and wind in the extratropical Northern Hemisphere agrees fairly well with observations. The day-to-day variability of the circulation also appears to be rather well simulated, with midwinter warmings of realistic intensity and suddenness appearing in the polar regions. The major deficiency is the absence of a realistic quasi-biennial oscillation (QBO) in the simulated winds in the tropical lower stratosphere. There is also an indication of long period (~10 year) variability in the winter polar vortex. This appears not to be related to any obvious source of long-term memory in the atmosphere such as surface boundary conditions or the flow in the tropical stratosphere.

The model has also been run through a large number of boreal winter simulations with imposed perturbations. In one set of experiments the Pacific sea surface temperatures have been changed to those appropriate for strong El Niño or La Niña conditions. The model is found to reproduce the observed extratropical stratospheric response to El Niño conditions quite well. Interestingly, the results suggest that including the interannual variations in SST would not greatly enhance the simulated interannual variance of the extratropical stratospheric circulation.

Another set of integrations involved arbitrarily altering the mean flow in the tropical lower stratosphere to be appropriate for different extremes of the QBO. The effect of these modifications on the simulated zonal-mean circulation in the extratropical winter stratosphere is found to be quite modest relative to that seen in comparable observations. The model results do display a clear effect of the imposed tropical lower-stratospheric wind perturbations on the extratropical summer mesospheric circulation. This could reflect the influence of the mean flow variations on the gravity waves forced in the Tropics, propagating upward and poleward and ultimately breaking in the extratropical mesosphere. The model behavior in this regard may be related to reported observations of an extratropical mesospheric QBO.

The equilibration of the stratospheric water vapor field in the long SKYHI control integration is examined. The results suggest that the mean residence time for upper-stratospheric air in the model is about 4 years.

1. Introduction

The Northern Hemisphere (NH) winter stratospheric circulation is notable for its very strong interannual variability. The standard deviation of monthly mean, zonal-mean temperatures at midstratospheric levels exceeds 10°C near the North Pole. This level of temperature variability is associated with large day-to-day changes in the flow in the polar vortex, most notably the major midwinter sudden warmings. The strong variability in the temperature and flow fields has important implications for modeling of trace constituents in the middle atmosphere. It is known that the flow evolution during a sudden warming has strong influence on the transport of ozone to high latitudes (e.g., Leovy et al. 1985). The variability of temperature is also likely to play a critical role in modeling the extent of polar stratospheric cloud formation (and consequent ozone depletion) in the Arctic (e.g., Austin et al. 1992). Thus, the simulation of the interannual and day-to-day variations of the NH circulation is a crucial issue for comprehensive general circulation models (GCMs) designed for the middle atmosphere.

Historically the development of stratospheric/mesospheric GCMs has not proceeded as quickly as for those dealing with only the lower atmosphere. Comprehensive model simulations have often been plagued by a cold bias in the high-latitude winter middle atmosphere (e.g., Manabe and Mahlman 1976). In the NH this problem has been significantly ameliorated in several models discussed over the last decade, either through incorporation of a parameterized subgrid-scale gravity wave drag (e.g., Rind et al. 1988a; Boville 1991) or, in the case of the GFDL SKYHI model,

Corresponding author address: Dr. Kevin Hamilton, GFDL/NOAA, Princeton University, P.O. Box 308, Princeton, NJ 08542.

through increasing the horizontal resolution (Mahlman and Umscheid 1987; Hamilton et al. 1995). When a reasonable simulation of the time-mean state is achieved, an examination of the variability of the model circulation is warranted. Boville (1986) addressed this issue using a 350-day perpetual January simulation with his spectral GCM, and Rind et al. (1988b) explored the interannual variability present in a 5-year seasonal integration with the GISS gridpoint climate model. The first part of the present paper discusses the day-to-day and interannual variability seen in a very long control run performed with the GFDL SKYHI general circulation model. Attention is restricted to the NH winter where the stratospheric variability is particularly pronounced. The SKYHI model control integration considered is briefly described in section 2, and the analysis of the variability in the simulated middle-atmospheric circulation is reported in section 3.

As in most earlier GCM studies of the stratospheric circulation, the control SKYHI integration discussed here employs climatological sea surface temperatures. It is well known that the interannual fluctuation of sea surface temperature (SST) has important effects on the tropospheric circulation, and so it is natural to consider the role of SST variability in the middle atmosphere as well. In the troposphere a rather complete GCM study of this issue by means of very long integrations with historically observed time series of global SST has been performed (Lau and Nath 1990). This approach with the high vertical resolution SKYHI model is too demanding on computer time to be practical at present. However, in this paper a first step will be taken by investigating the effects of idealized SST perturbations in the tropical Pacific. These model experiments are described in section 4.

One deficiency that has apparently affected all published comprehensive atmospheric circulation model simulations is the unrealistically small amplitude of the quasi-biennial variability in the tropical stratosphere (e.g., Hamilton and Yuan 1992; Cariolle et al. 1993; Hamilton et al. 1995). Since the quasi-biennial oscillation (QBO) is thought to affect the NH extratropical stratospheric circulation, this may be an important limitation for the present study of NH interannual variability. As part of the present project, the NH extratropical circulation is examined in a series of SKYHI integrations with arbitrary momentum forcing imposed to drive the tropical stratosphere toward the QBO extremes. These results are discussed in section 5.

In addition to the examination of the year-to-year variability in the model, this paper will also take advantage of the existence of the very long SKYHI control integration to look at the equilibration of the simulated stratospheric water vapor field. This is an issue of great importance for the development of comprehensive 3D models of middle atmospheric photochemistry, and the present control SKYHI integration allows a rather direct examination of this process. This issue is considered in section 6.

Further discussion of the present findings and the conclusion to the paper are included in section 7. Note that some preliminary aspects of the results in this paper have been presented in Hamilton (1993a,b, 1994). Strahan and Mahlman (1994a,b) discuss some aspects of the stratospheric interannual variability in a much shorter control integration with a higher horizontal resolution (1° × 1.2° latitude–longitude) version of the SKYHI model.

2. Model and control integration

The description of the SKYHI model and some control integrations with a prescribed seasonally varying SST field are contained in a companion paper (Hamilton et al. 1995, hereafter HWMU). In the present paper attention will be restricted to simulations with the 3° × 3.6° 40-level version. As noted in HWMU, this control run began from initial conditions interpolated from the end of an almost yearlong integration with a higher-resolution version of the model. The dating system used for the SKYHI results is also explained in section 2 of HWMU. More than two years of the 3° × 3.6° SKYHI integration were discarded before the analysis period to be considered here. Most of the analysis included here is based on 25 boreal winters of data (*1985/86* through *2009/10*) (hereinafter italic font will denote model years). Another 4 winters are now available, and these will be included in the examination of long-term trends described in the following section. As noted earlier, one model deficiency of obvious relevance for the present paper is the virtual absence of a QBO in the tropical stratosphere of the SKYHI model (see HWMU). Brief descriptions of the observational datasets used here for comparison purposes are also given in HWMU.

3. Variability in the control run

Figure 1 shows the standard deviation of the monthly mean, zonally averaged temperature for each of December, January, and February in the SKYHI control run and in observations [Randel (1992), available only up to 1.0 mb]. In each month the standard deviation in the model is strongly concentrated in the high-latitude upper stratosphere and mesosphere. This polar concentration of the variance is also apparent in the observations. However, the model results clearly show that the variability in the NH polar region in December is greater than in January or February (at least above 10 mb), while Randel's observational analysis suggests that December temperatures actually have lower interannual variability. The net result is that the model and observations agree quite well in January and February, while the model quite significantly overestimates the standard deviation in December between 10 and 1 mb.

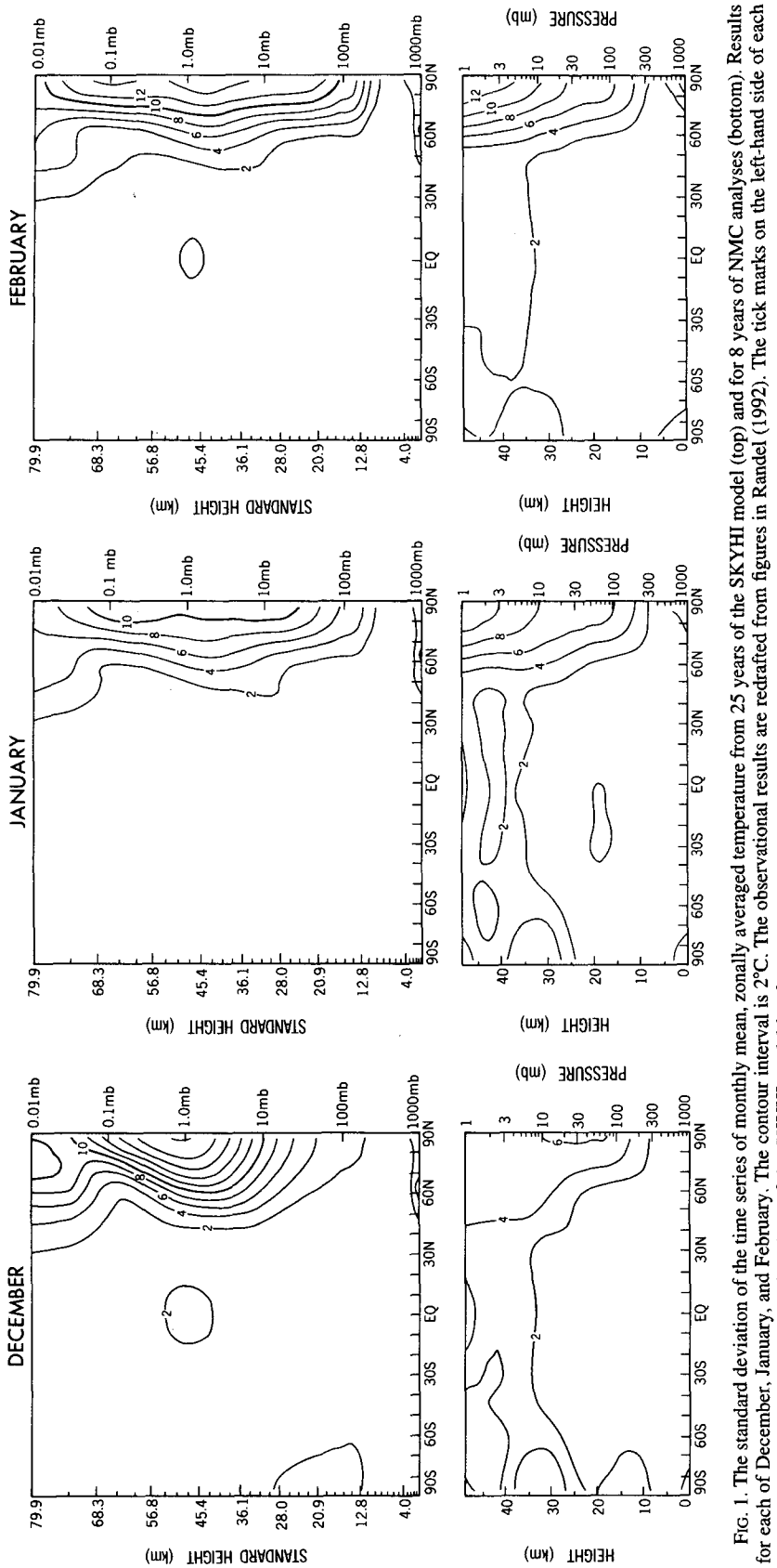

FIG. 1. The standard deviation of the time series of monthly mean, zonally averaged temperature from 25 years of the SKYHI model (top) and for 8 years of NMC analyses (bottom). Results for each of December, January, and February. The contour interval is 2°C. The observational results are redrafted from figures in Randel (1992). The tick marks on the left-hand side of each of the top row of panels show the locations of the SKYHI model levels.

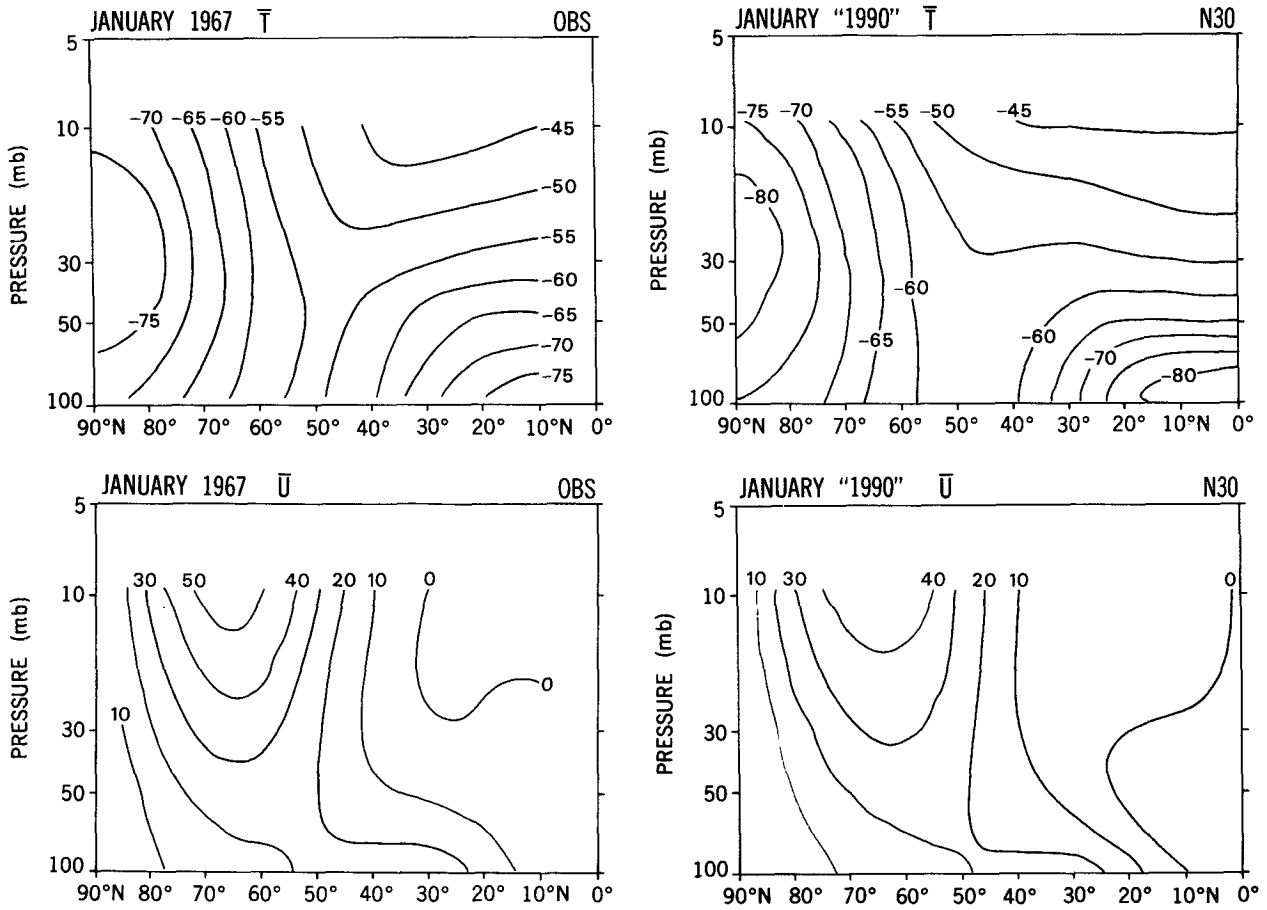

FIG. 2. The zonal-mean temperature and zonal wind fields averaged over January. Results for observations in 1967 (left panels) and for model year *1990* from the N30 SKYHI control run (right panels). The observational results are redrafted from van Loon et al. (1972).

Below 10 mb the agreement between SKYHI and the observations in December (as well as in January and February) is reasonably good.

In low latitudes and in the summer (Southern) hemisphere there is a definite difference between the model results and observations in all three months, with the observed standard deviation being larger than that in the model almost everywhere. Thus, for example, in February the observed standard deviation in Fig. 1 is between 2° and 4°C above 10 mb everywhere between 60°S and 60°N. In the model the standard deviation exceeds 2°C only in a tiny region right near the equator at 1 mb. To some extent, this difference may reflect real deficiencies in the model dynamics (notably the virtual absence of a quasi-biennial oscillation; see HMWU). However, the observations themselves in these regions of rather small variance need to be regarded with caution. The NMC operational analyses used by Randel could be subject to long period inhomogeneities due to changes in satellite instruments and analysis procedures. Such problems would introduce spurious contributions to the observed interannual variance. There is also likely a significant component of interannual variability in tropical and summer temperatures resulting from changes in atmospheric composition (notably volcanic aerosols) and solar flux in the real world that have no counterpart in the SKYHI control integration.

Figure 1 presents a nice view of the overall magnitude of the interannual variability in the NH winter middle atmosphere. Now consideration will be given to more detailed aspects of the simulation of the NH winter variability in SKYHI. Examining 8 years of lower-stratospheric NH analyses from the Free University of Berlin (FUB), van Loon et al. (1972) produced temperature and zonal wind cross sections for their least disturbed (i.e., coldest pole) January and for the most disturbed (warmest pole) January. These results are reproduced as the left-hand panels of Figs. 2 and 3 for the "cold" January (1967) and the "warm" January (1968), respectively. For comparison, 8 consecutive years of the present control SKYHI simulation were examined. The wind and temperature cross sections for the "coldest" January (*1990*) and the

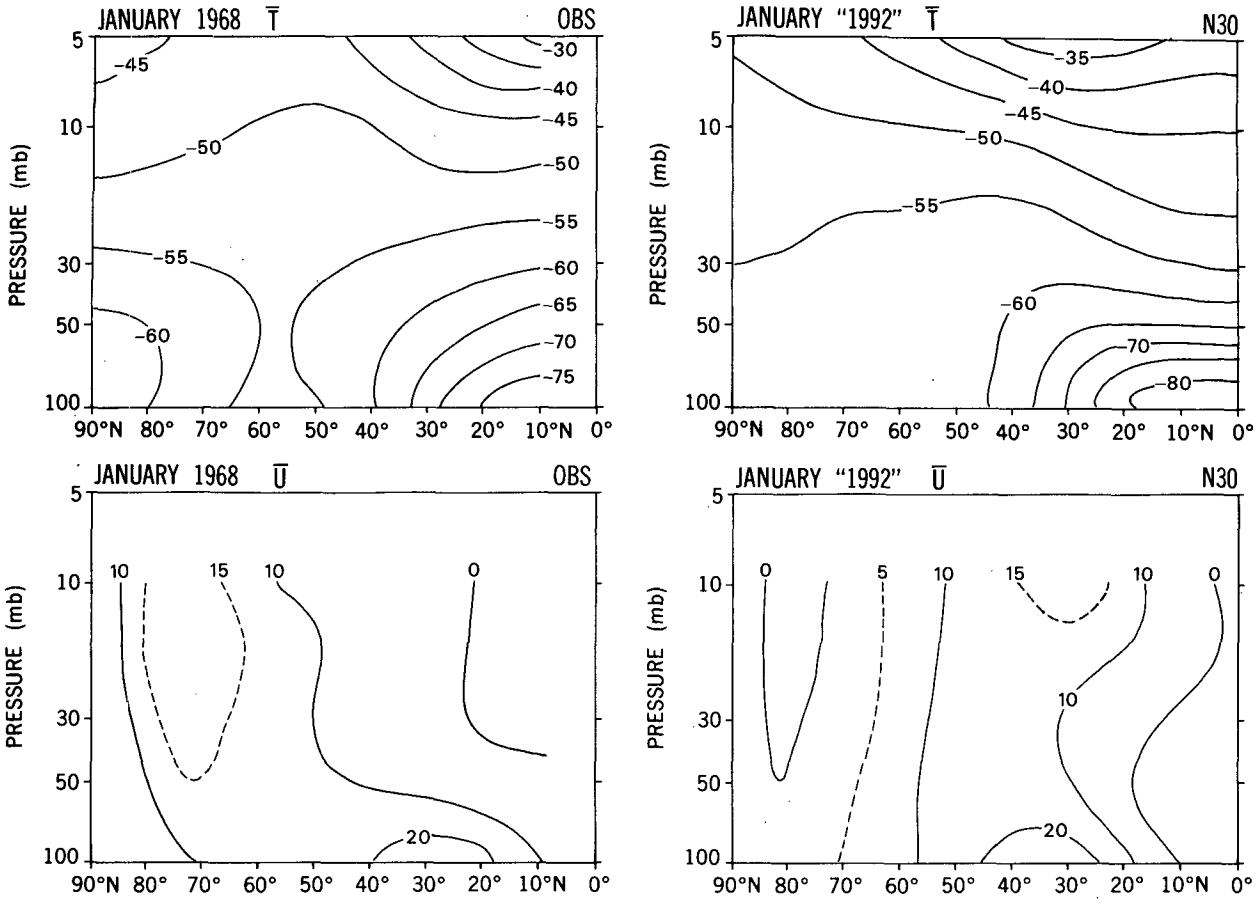

FIG. 3. As in Fig. 2 but observations are from 1968 and the SKYHI results are from model year *1992*.

"warmest" January (*1992*) are shown in the right-hand panels of Figs. 2 and 3. The similarities between the model and observed cross sections in each pair are evident (temperatures for the most part within 5°C). It is apparent that the SKYHI model can display roughly the same range of variability in the monthly mean NH winter lower-stratospheric circulation as does the real atmosphere.

Figure 4, reproduced from Naujokat et al. (1988), shows another observational characterization of the variability in the NH winter stratosphere. Daily time series of the 30-mb North Pole temperature are plotted for the November–April period in 10 consecutive years [plots for a number of additional years can be found in Naujokat et al. (1988)]. The dotted curve in each panel is exactly the same and represents the long-term (>20 year) mean for each calendar day. Periods of anomalously warm temperatures are denoted by shading. These observed North Pole temperatures are from the FUB subjectively analyzed NH analyses based on radiosonde data. Figure 4 shows some rather undisturbed winters (such as 1982/83 or 1985/86), which are characterized by anomalously cold temperatures most of the time, interrupted only by small amplitude high-frequency variability. By contrast, there are also winters that obviously were affected by major sudden warmings. The polar temperature in the strongest warming events (February 1979, February 1984, December 1984/January 1985, January 1987) rises 35°–40°C in a period of 5–8 days. The polar temperature tends to remain anomalously warm for at least the next month, and the occurrence of a warming in a particular year will significantly impact even the winter mean temperature. Figure 5 shows the same 30-mb temperature time series, but for 10 consecutive years of the SKYHI control run. To first order the model results are very encouraging. In particular, about half the model winters have warmings of realistic amplitude and suddenness. On closer inspection some differences in the details of the temperature time series in model and observations do appear. The "cold" winters in the SKYHI simulation (e.g., *1986/87* or *1994/95*) tend to be even more undisturbed than the coldest observed winters. In fact there is a general lack of high-frequency, small amplitude warming events in the model relative to those found in the observed time series. As noted above, the

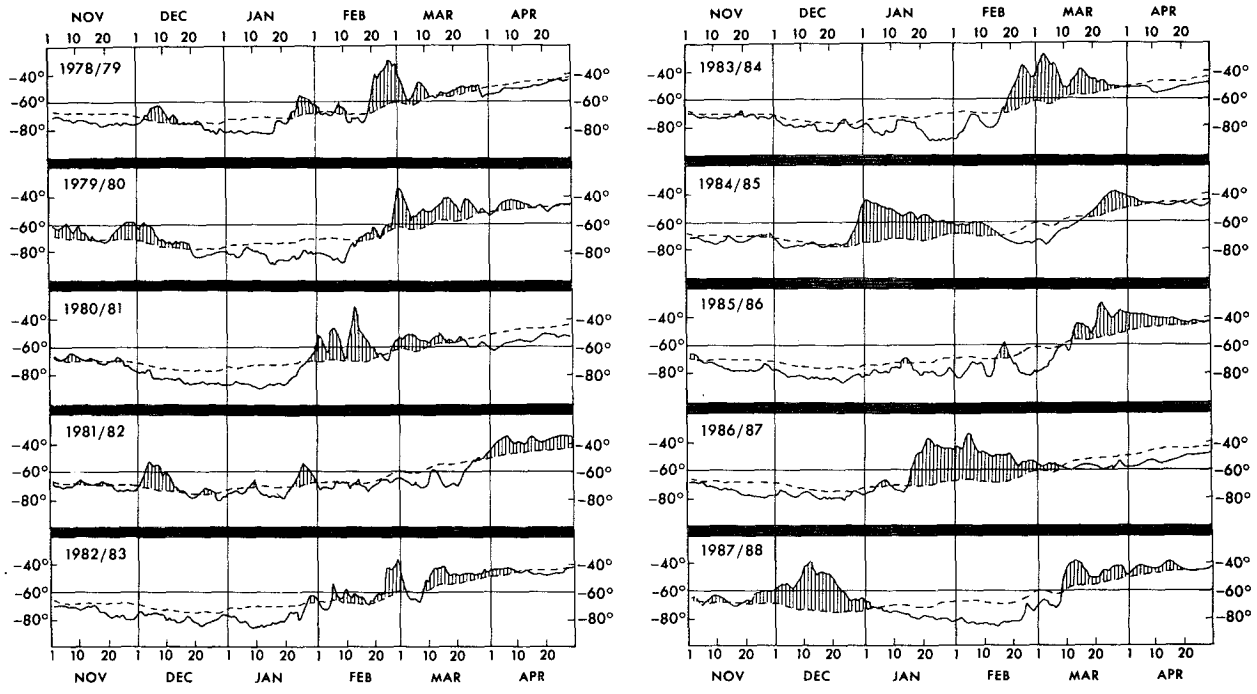

FIG. 4. Time series of observed daily 30-mb North Pole temperatures for November–March of 10 consecutive years. The dashed lines give the long-term mean values for each calendar day. Anomalously warm periods are denoted by shading. The temperature labels are in degrees Celcius. Redrafted from Naujokat et al. (1988).

major warming events are about as frequent in the simulation as in observations, but there seems to be a bias for the model to have more warmings in the early winter. In fact, Fig. 5 shows that strong warmings occurred in December *1990/91, 1991/92,* and *1992/93.* This is consistent with the earlier result in Fig. 1, which suggested that the model significantly overestimates the interannual variability of the December temperatures in the upper stratosphere.

The detailed model behavior in the midwinter warming events is still being investigated and will be discussed in a future paper. Preliminary analysis suggests that the evolution of individual sudden warmings is quite realistic. As an example, Fig. 6 shows the progression of the 10-mb height field through the warming seen in early January *1989.* The very strong zonal wave 2 warming is evident. The evolution of the 10-mb heights in this model event is quite similar to that in the observed February 1979 sudden warming, which has been documented in Andrews et al. (1987; see their Figure 6.3 showing the 10-mb heights). The February 1979 vortex breakdown was a predominantly wave 2 event, and it proceeded just as rapidly as the model warming illustrated in Fig. 6 (compare the evolution in shown in Andrews et al. during 19–26 February with that in the model during 5–13 January). The warmings in the model also display a reasonably realistic vertical structure, with a rapid downward propagation of the zonal-mean warming generally evident.

The geographical distribution of variability in the seasonal-mean circulation is explored in Figs. 7 and 8. In particular, Fig. 7a shows the standard deviation of the DJF mean 50-mb heights computed from 25 years of SKYHI simulation. This is compared in Fig. 7b to an observational estimate of the same quantity based on 34 years of the FUB analyses. The results in Fig. 7b are reproduced from Hamilton (1993c) and actually represent the interannual variance in a time series that has been slightly modified in order to remove the effects of the tropical QBO [without this modification the pattern is similar but the values are very roughly 10% higher; see Hamilton (1993c)]. Both model and observations show a distribution of the standard deviation centered near the pole, but stretched in a wave 2 pattern so that the maximum variability lies along an axis very roughly aligned with the 90°E–90°W meridian. The peak values and the meridional gradients near the pole are both larger in the model results than in observations. Figures 8a and 8b show the same comparison at 30 mb. While the overall agreement between model and observations is still apparent, the unrealistically strong polar intensification of variability is more pronounced at 30 mb than at 50 mb. This seems consistent with the bias extensively documented in HWMU for the SKYHI polar vortex itself to be too strongly confined to high latitudes, particularly in the upper stratosphere and mesosphere.

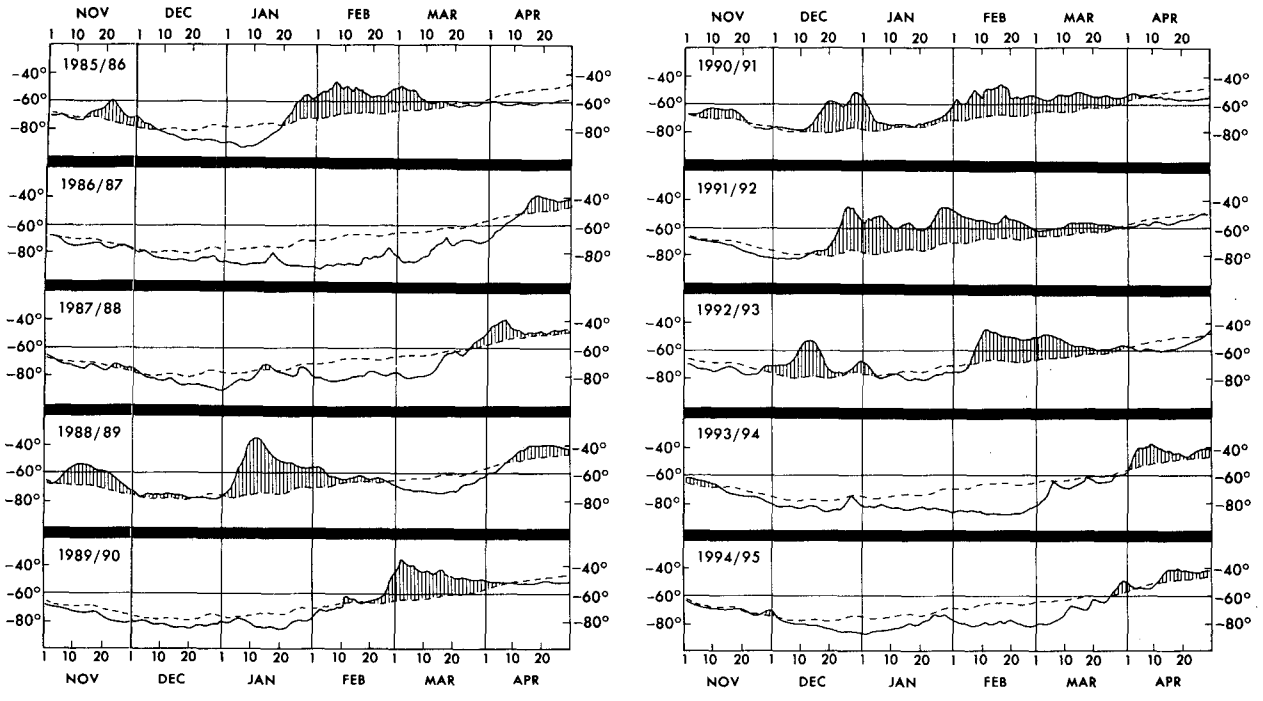

FIG. 5. As in Fig. 4 but for 10 consecutive years of the SKYHI control integration.

One interesting feature seen in the model-simulated 30-mb polar temperatures shown in Fig. 5 is the occurrence of 5 consecutive warm winters (*1988/89* through *1992/93*). This contrasts with the rough tendency in the real atmosphere for warm and cold winters to alternate (e.g., Fig. 4). Figure 9 shows the SKYHI DJF North Pole temperatures in 29 consecutive years at several stratospheric levels. The rather long-term variability in these temperatures is apparent. Indeed, one is tempted to identify a rather regular 10-year cycle in these series, particularly in the first 20 years of the record. This period is close to that of the familiar cycle of solar activity, and it is conceivable that the reported observations of solar effects in the stratospheric polar temperatures (e.g., Labitzke 1987) really reflect the internal variability of the atmosphere similar to that seen in the present model simulation. Of course, in the real world, the polar stratospheric temperatures also have a pronounced biennial character (possibly influenced by the tropical QBO), which is missing from the SKYHI simulation.

The low-frequency variability seen in Fig. 9 is surprising, since the conventional view is that long-term memory in the atmospheric circulation must reside in the lower boundary condition, and most significantly in the SST field. In the present case the SSTs (and sea ice) are prescribed to climatological values, so that the only interannual fluctuations in the lower boundary condition are in the soil moisture. It seems rather implausible that the soil moisture variations could really account for the large variability seen in Fig. 9, and so the question of where the memory for the system resides is still open. An obvious possibility for the repository of memory is the tropical lower stratosphere. In this region, the effective radiative constraint on the zonal-mean circulation is weak (due to the long radiative timescales and the small Coriolis parameter), and the strong static stability insulates the flow from the mechanical spindown associated with the coupling to the surface. Thus, a perturbation to the zonal-mean flow in the tropical lower stratosphere has the potential to persist for very long periods (hence the existence of the QBO itself in that region). Figure 10 shows the DJF equatorial zonally averaged zonal wind at 10 mb, 30 mb, 50 mb, and 100 mb. At 100 and 50 mb the variations are extremely small ($\sim$2 m s^{-1} total change over most of the record), while the variations are slightly larger at 30 and 10 mb. The evolution of equatorial mean flow in this figure to some extent reflects the very weak QBO documented in HWMU but also has a significant random component that certainly does not appear to be correlated with the polar temperature time series (Fig. 9). If there is some connection between the interannual fluctuations in the polar temperature and the mean wind in the tropical stratosphere, it must be a very subtle effect.

The low-frequency behavior seen in the SKYHI polar stratosphere has some similarity to recent results of James and James (1992), who found enhanced variability at periods from 5 to 40 years in very long in-

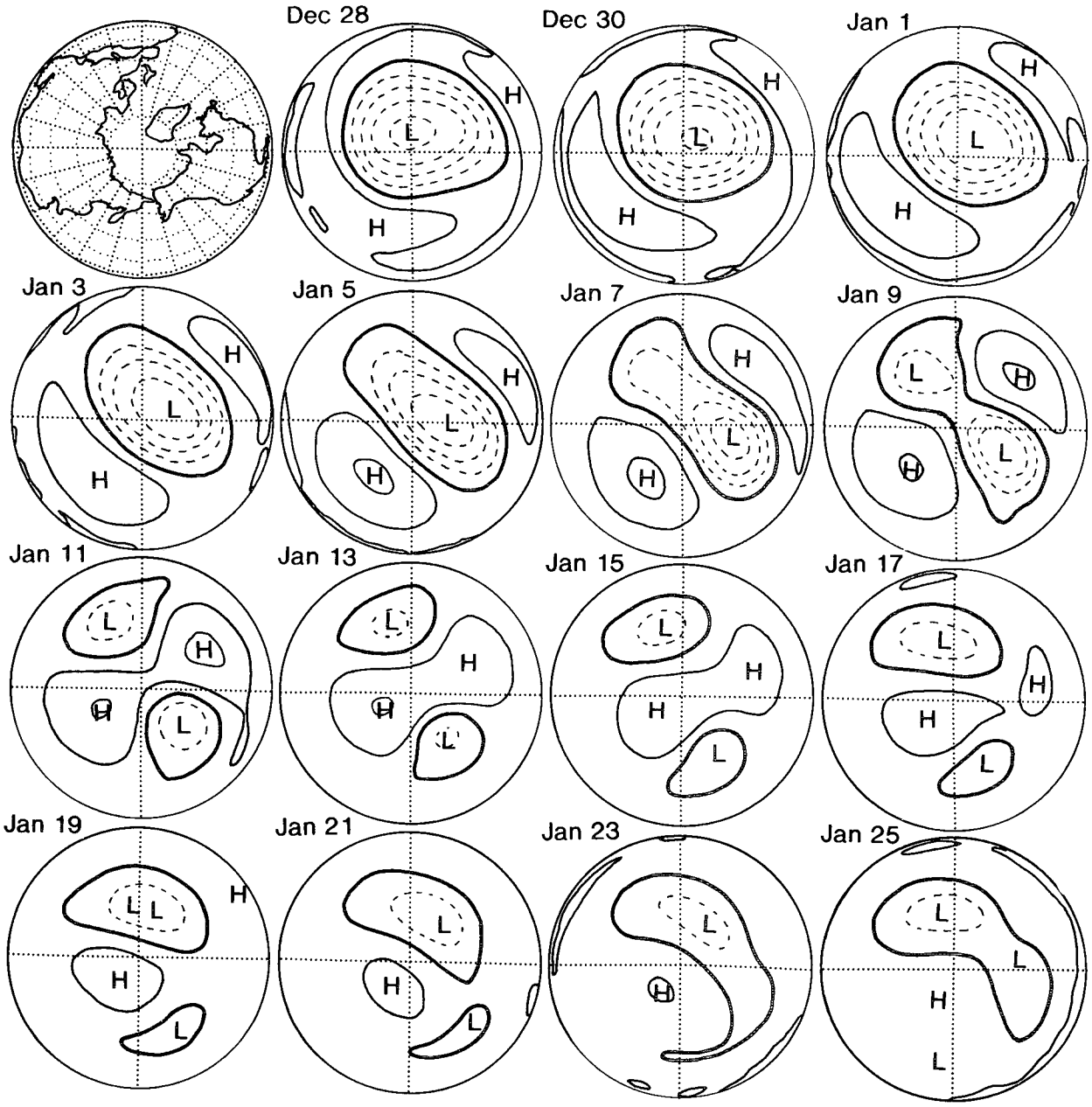

FIG. 6. Northern Hemisphere 10-mb heights at 2-day intervals from the SKYHI control integration during late *1988* and early *1989*. The contour interval is 500 m, and dashed contours are used for values below 30 km.

tegrations performed with a simplified tropospheric GCM. It is possible that the SKYHI model (with essentially fixed lower boundary condition) has similar tropospheric variability, which is then amplified in the stratosphere, leading to the extremely large signal seen in Fig. 9. It is fair to say, however, that neither the James and James results nor the low-frequency variability in the SKYHI integration are entirely understood at present.

4. Experiments with imposed tropical Pacific SST anomalies

The question of how the interannual variability in the stratosphere is affected by SST variations is an important one, particularly as most hitherto published simulations with stratospheric GCMs have employed climatological SSTs. There have been some observational papers on one aspect of this issue, namely, the

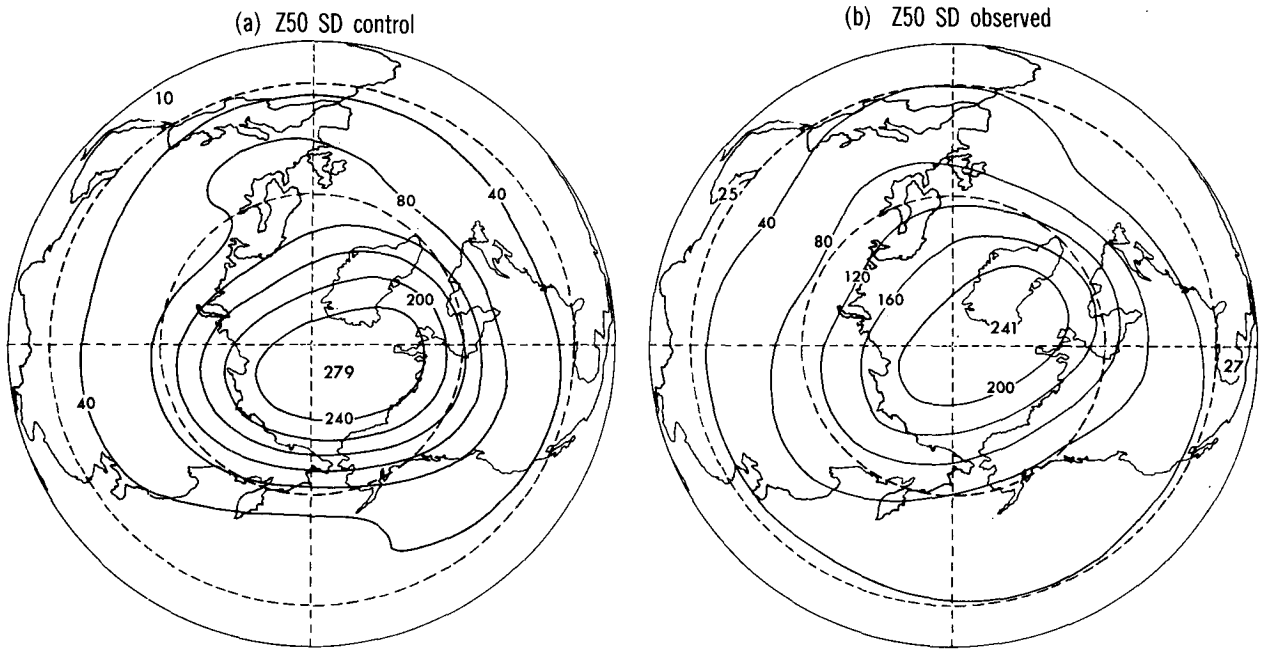

FIG. 7. The standard deviation of the December–February mean 50-mb height field. Results from (a) 25 years of the SKYHI control integration and (b) 34 years of observational analyses. Observational results reproduced from Hamilton (1993c). The dashed circles are at 30° and 60°N latitude.

effects of the familiar Southern Oscillation in the stratosphere; van Loon and Shea (1985), van Loon and Labitzke (1987), and Hamilton (1993c) have all examined NH winter mean stratospheric geopotential fields composited for the extremes of the Southern Oscillation (SO). The SO is associated with particularly strong and systematic variations in tropical Pacific SST that are known to greatly affect several aspects of the

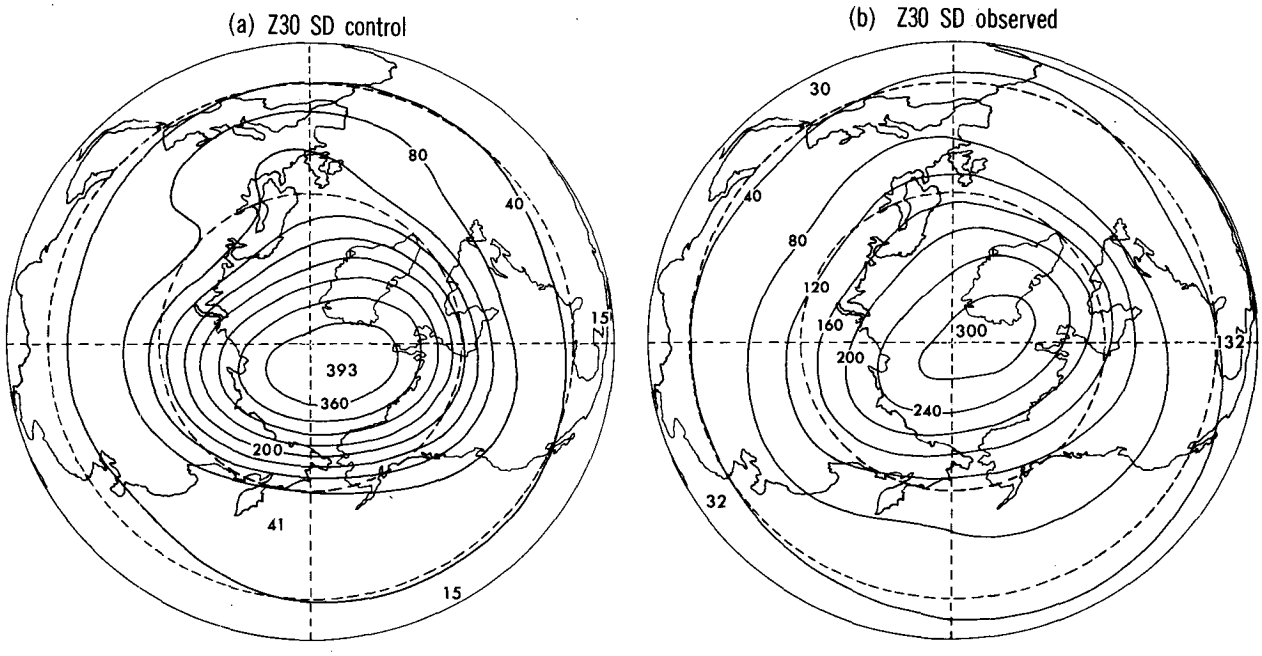

FIG. 8. As in Fig. 7 but for the 30-mb level.

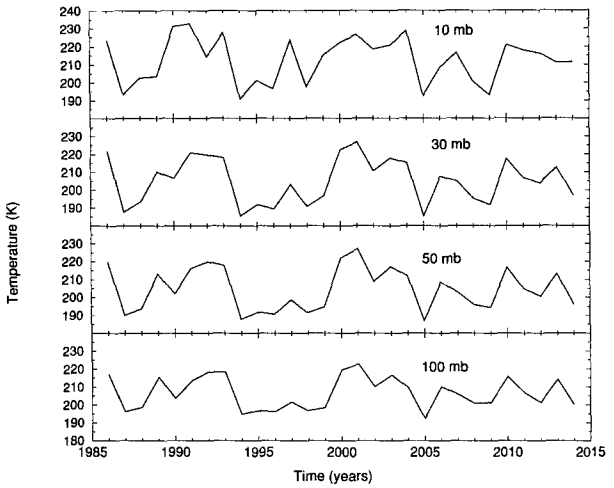

FIG. 9. The December–February mean North Pole temperature in each of 29 consecutive years from the SKYHI control run. Results for 10 mb, 30 mb, 50 mb, and 100 mb.

tropospheric circulation (e.g., van Loon and Madden 1981; Rasmusson and Carpenter 1982). The most complete examination of the stratospheric extension of the SO is by Hamilton (1993c), who found that the stationary wave pattern in the NH winter extratropical stratosphere is significantly affected by the phase of the SO, with the effects of warm extremes (El Niño events) being more pronounced than the cold extremes [La Niña events, in the terminology of Philander (1990)].

As part of the present study, an examination of the effects of Pacific SST anomalies in the SKYHI model was conducted. The 25 DJF periods from *1985/86* through *2009/10* serve as the control. Then, in the spirit of some earlier tropospheric GCM studies (e.g., Boer 1985), 10 warm anomaly perturbation integrations

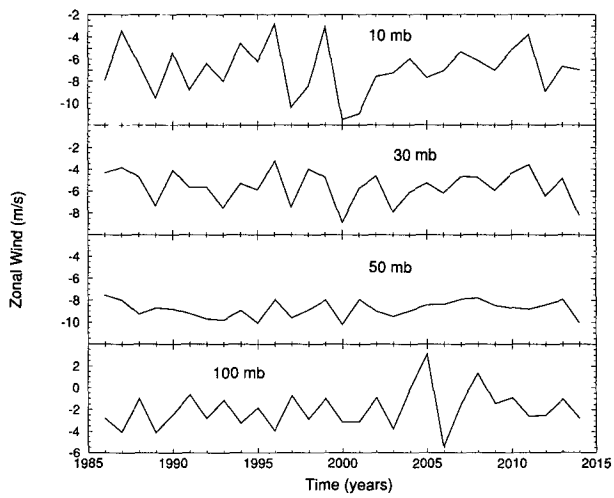

FIG. 10. As in Fig. 9 but for the equatorial zonally averaged zonal wind.

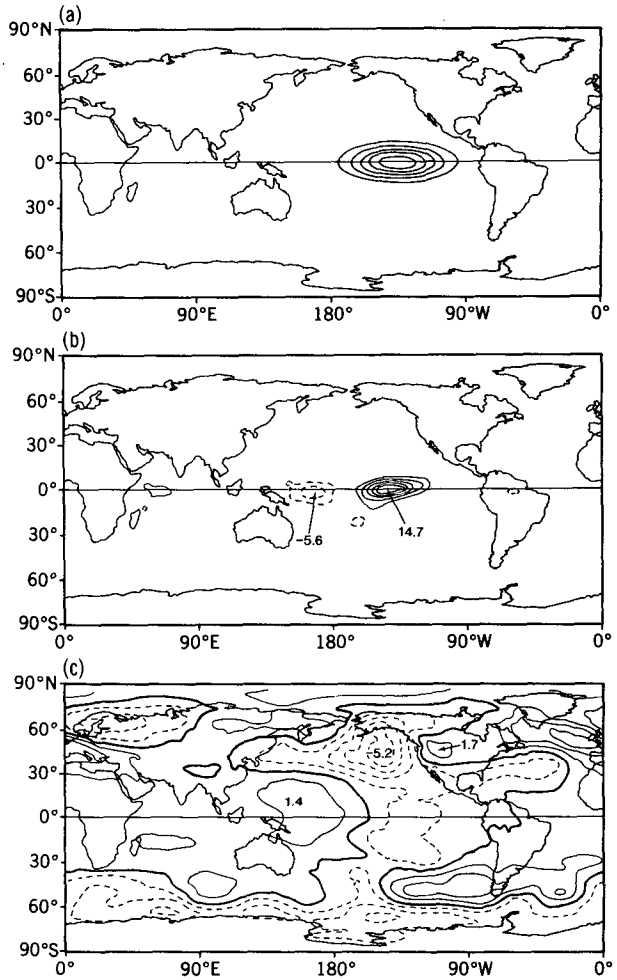

FIG. 11. (a) The sea surface temperature perturbation imposed in the warm-phase experiments. The contour interval is 0.5°C. (b) The December–February mean precipitation averaged over the 10 warm-phase experiments minus that in the 25-year control run. The contour interval is 2 mm d^{-1}, and dashed contours indicate negative values. (c) The December–February mean surface pressure averaged over the 10 warm-phase experiments minus that in the 25-year control run. The contour interval is 1 mb.

were performed, each starting from atmospheric initial conditions taken from 1 August of one of 10 consecutive years in the control integration. The anomaly employed is shown in Fig. 11a, and in each case it was imposed at full strength on 1 August and maintained throughout the integration. Each perturbation experiment extended for 7 months, and in each case the final 3 months (DJF) are analyzed. The shape of the SST perturbation was taken from Ting and Held (1990) and represents an idealization of the SST anomaly seen in the mature phase winter in the El Niño composite of Rasmusson and Carpenter (1982). The magnitude adopted (peak value of 3°C) is very large; it is appropriate for only the very strongest of observed El Niño events and is a factor of 1.5–2 larger than that observed

in the mature phase of typical events. The imposition of the full magnitude of the anomaly starting in August is somewhat unrealistic and may also contribute to an artificial enhancement of the SST effects in the model simulations relative to those in typical observed El Niño events. These 10 warm anomaly simulations were then supplemented by 10 integrations, which were identical except that the sign of the imposed Pacific SST anomaly was negative.

a. Tropospheric effects

Figure 11b shows the DJF precipitaiton averaged over the 10 El Niño perturbation runs minus that averaged over the 25 control winters. The strong effects of the imposed warm pool are evident, with weaker rainfall than normal in the western equatorial Pacific and anomalously heavy rainfall in the central Pacific. This effectively amounts to an eastward shift of the principal region of heavy precipitation in the equatorial Pacific and is in general agreement with observations during an El Niño event (e.g., Philander 1990). Figure 11c shows the DJF surface pressure in the warm perturbation experiments minus that in the control run. Along the equator one sees the anomalous high pressure in the western Pacific and anomalous low pressure in the eastern Pacific. Table 1 summarizes the DJF surface pressure data at the model grid points nearest to Tahiti and Darwin in the control and in the warm and cold anomaly experiments. An average drop of 2.5 mb in the usual Tahiti–Darwin Southern Oscillation index (SOI) (e.g., Philander 1990) is found in response to the warm SST perturbation. The 2.5 mb is comparable to the decline seen in the SOI during extremely strong ENSO events in real data.

The effects of the warm SST anomaly on the model surface pressure are also clearly felt off the equator, and in a rather realistic fashion. In particular, the appearance of anticyclones on either side of the equator west of the warm anomaly, the intensification of the Aleutian low, and the occurrence of anomalously high pressure over much of Canada and the northwest United States are also apparent in observations (e.g., van Loon and Madden 1981). These general aspects of the model response appear quite clearly when only half of the 10 perturbation experiments are included in the composite (or when only 10 of the 25 control winters

TABLE 1. Surface pressure at grid points near Tahiti and Darwin. DJF means for control, warm SST anomaly, and cold SST anomaly cases.

Experiment	16.5°S, 149.4°W	13.5°S, 131.4°E	Tahiti − Darwin
Control	1010.82	993.16	17.66
Warm	1009.28	994.14	15.14
Cold	1012.30	992.22	20.08

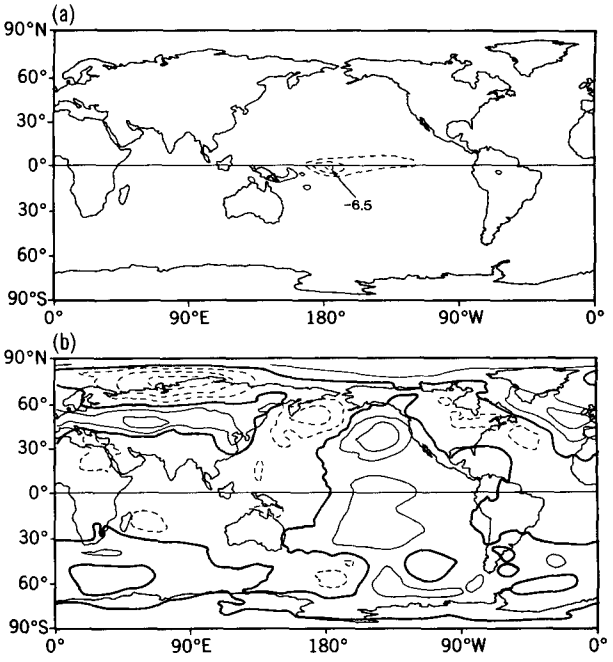

FIG. 12. (a) The December–February mean precipitation averaged over the 10 cold-phase experiments minus that in the 25-year control run. The contour interval is 2 mm d^{-1}, and dashed contours indicate negative values. (b) The December–February mean surface pressure averaged over the 10 cold-phase experiments minus that in the 25-year control run. The contour interval is 1 mb.

are used). Hamilton (1988) found that the maximum intensification of the Aleutian low in a composite over 15 ENSO events observed in the twentieth century was between 3 and 4 mb. The maximum 5.2 mb anomaly in Fig. 11c is thus reasonable, given the very strong SST warming imposed.

Figure 12 summarizes the surface response to the cold (La Niña) SST anomaly. Figure 12a shows the DJF precipitation in the 10 cold anomaly experiments minus that in the control. As might be expected, the effects are roughly opposite to those seen in the warm case, with the rainfall along the equatorial central Pacific reduced in the La Niña experiments. However, the La Niña precipitation anomaly is considerably weaker than that for the El Niño integrations, and the location of the anomaly is rather different. While the positive El Niño rainfall anomaly peaks at about 150°W, the negative La Niña anomaly is largest near 180°. This asymmetry between the rainfall response to warm and cold anomalies may largely reflect the smallness of the central Pacific rainfall in the neutral phase of the SO.

The weakness of the cold anomaly response is also seen in the extratropical surface pressure field shown in Fig. 12b. This has roughly the opposite sign of El Niño pressure anomaly (Fig. 11c), particularly in the eastern Pacific, but is only about half as intense. There does not appear to be any published La Niña composite that can be directly compared with this. At low latitudes

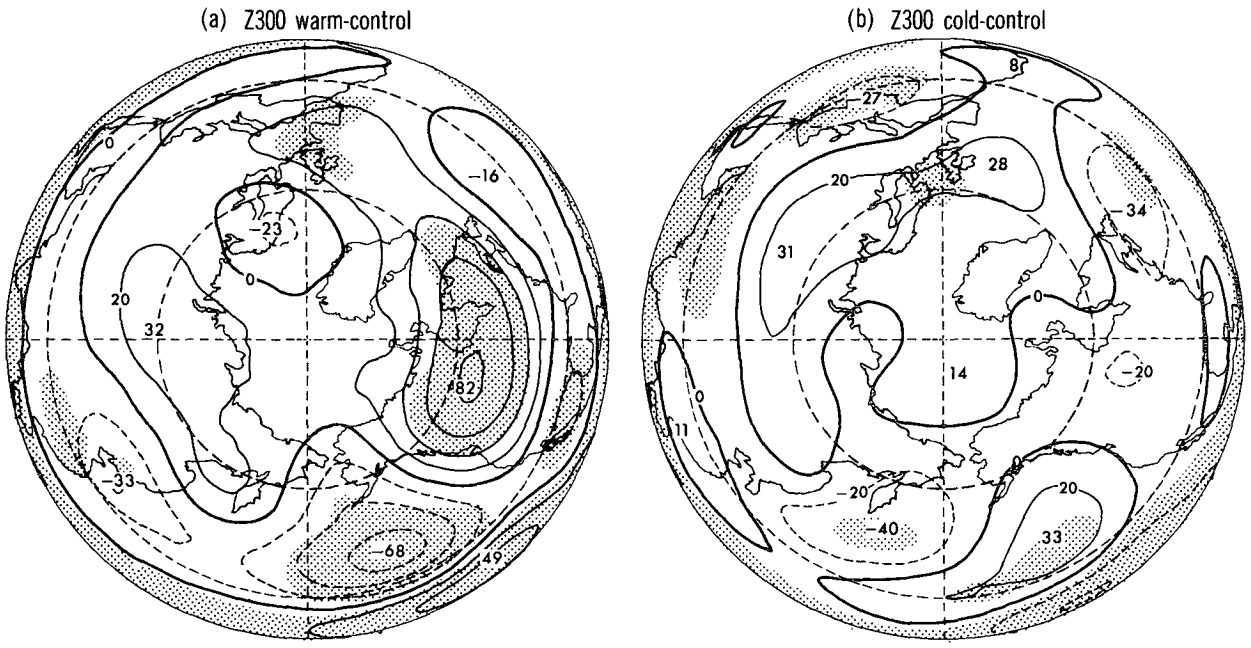

FIG. 13. (a) The December–February mean 300-mb height field averaged over the 10 warm phase experiments minus that in the 25-year control run. The contour interval is 20 m, and dashed contours indicate negative values. The shaded areas are regions where the results are judged significantly different from zero using a 95% criterion in a two-tailed t test. (b) As in (a) but for the 10 cold-phase experiments minus the results from the 25-year control run.

the pressure anomaly in the cold integrations more nearly matches that of the warm anomaly case. Table 1 shows that the DJF Tahiti–Darwin SOI is almost 2.5 mb higher in the La Niña experiments than in the control. In fact, the results in Table 1 indicate a peak-to-peak swing in the SOI of almost 5 mb. This is somewhat larger than observed, but this result may be understood as a consequence of the strength of the SST anomalies imposed in the model experiments.

Figure 13 shows the DJF anomalies in the NH upper-tropospheric geopotential field in the El Niño experiments (panel a) and the La Niña experiments (panel b). Just as at the surface, the warm SST perturbation produces a cyclonic 300-mb anomaly over the Pacific and an anticyclonic anomaly over North America, while the cold SST perturbation produces roughly the opposite (though much weaker) response. This is in general agreement with observational studies of the relation between upper-tropospheric geopotential and tropical Pacific SST (e.g., Pan and Oort 1983).

b. Stratospheric effects

Figure 14 shows the DJF mean horizontal wind anomalies in the warm SST perturbation experiments at levels in the upper troposphere and lower stratosphere. At 210 mb the dominant signal is the pair of strong anticyclonic circulations on either side of the equator in the eastern Pacific. By 103 mb the tropical Pacific signal is much weaker (note the factor of 4 difference in the scaling of the arrows), and the most organized wind anomalies are in the cyclonic circulation over the North Pacific and east Asia and in the anticyclonic circulation over North America. This pattern is even more pronounced at the next highest model level (81 mb). Here the equatorial wind anomalies are almost all less than 1 m s^{-1} and are completely overshadowed by the extratropical circulations. Thus, the direct penetration of the SST-induced signal into the tropical stratosphere is extremely weak. This result stands in contradiction to speculations that the tropical SST variability might be responsible for some of the strong quasi-biennial variability seen in the equatorial stratosphere (e.g., Brier 1978). The present model result is consistent with recent empirical studies that have found no significant link between the stratospheric QBO and the quasi-biennial component of the SO (Barnett 1991).

The smallness of the stratospheric influence from the SST perturbation is not entirely unexpected. The linear theory of vertically propagating equatorial waves (e.g., Andrews et al. 1987) suggests that vertical wavelengths and vertical group velocities will become very small as the zonal wave phase speed approaches the mean flow velocity. Given the weakness of the mean flow, linear stationary waves in the tropical lower stratosphere should thus be damped very rapidly in the vertical. In the troposphere, longitudinally varying stationary features such as the Walker circulation can thrive due to in situ thermal forcing as well as frictional (small-scale

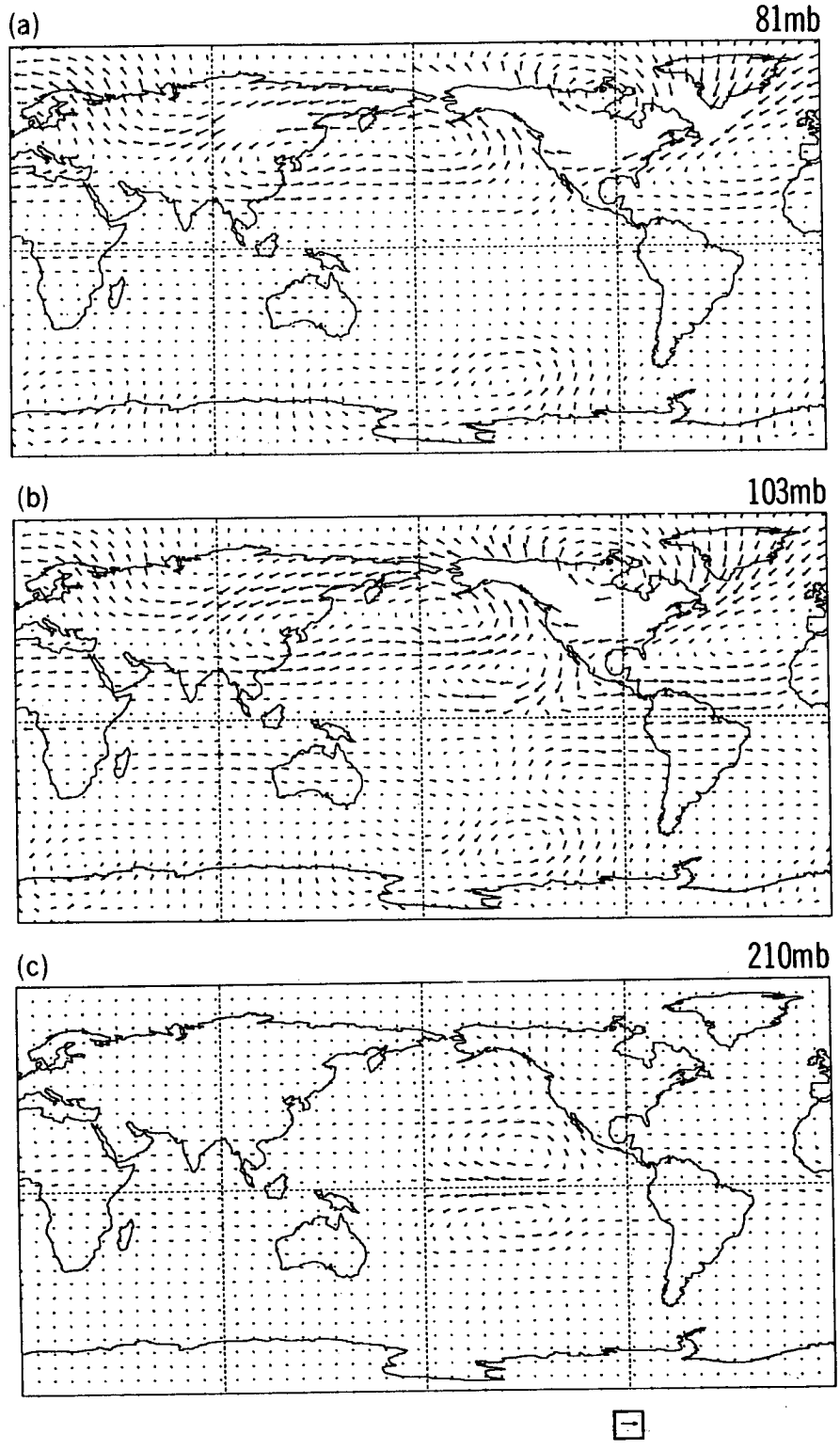

FIG. 14. December–February mean horizontal wind averaged over the 10 warm-phase perturbation experiments minus that in the control integration. Results for model levels at (a) 81, (b) 103, and (c) 210 mb. The arrow in the box in the lower right-hand corner represents 4 m s^{-1} in (a) and (b) and 16 m s^{-1} in (c). For clarity of presentation no vectors are plotted at points where the wind speed exceeds that indicated by the arrow in the lower right-hand corner.

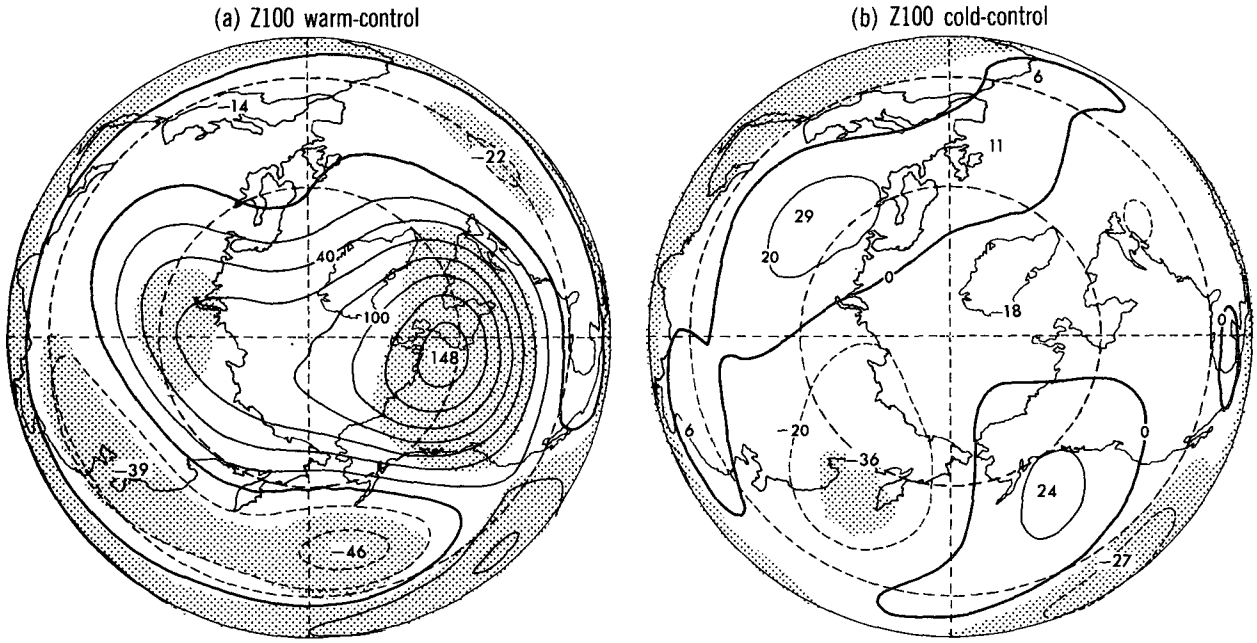

FIG. 15. As in Fig. 13 but for 100-mb heights.

mixing) effects. Any stratospheric extension of these features will have dynamics that must be reasonably well described by unforced linear wave theory. Thus, the direct tropical penetration into the stratosphere can be expected to be limited. The interesting aspect of the present numerical simulation is the demonstration of

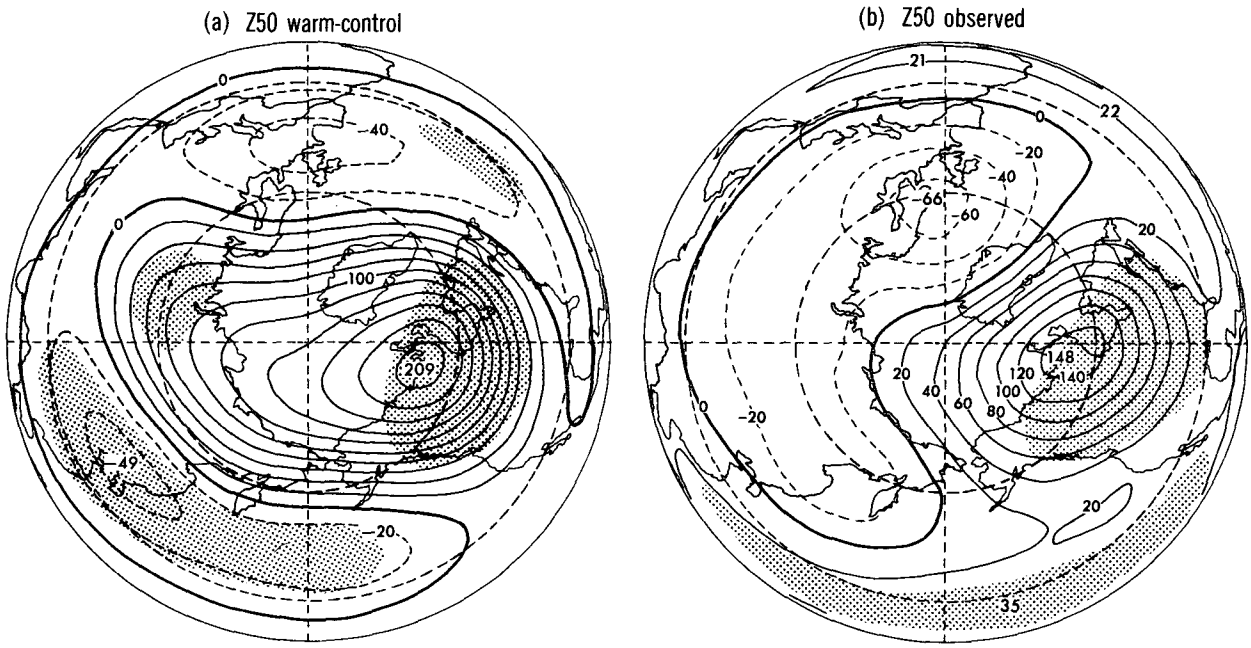

FIG. 16. (a) The model-simulated December–February 50-mb height averaged over the 10 warm-phase experiments minus that in the 25-year control run. (b) The difference between the observed December–February 50-mb geopotential height averaged over 9 mature phase El Niño winters minus the average over 18 "normal" winters (i.e., winters in which the SO was in neither its warm or cold extreme). See Hamilton (1993c) for further details. In each case the contour interval is 20 m, and negative values are represented by dashed contours. The shaded areas are regions where the results are judged significantly different from zero using a 95% criterion in a two-tailed t test.

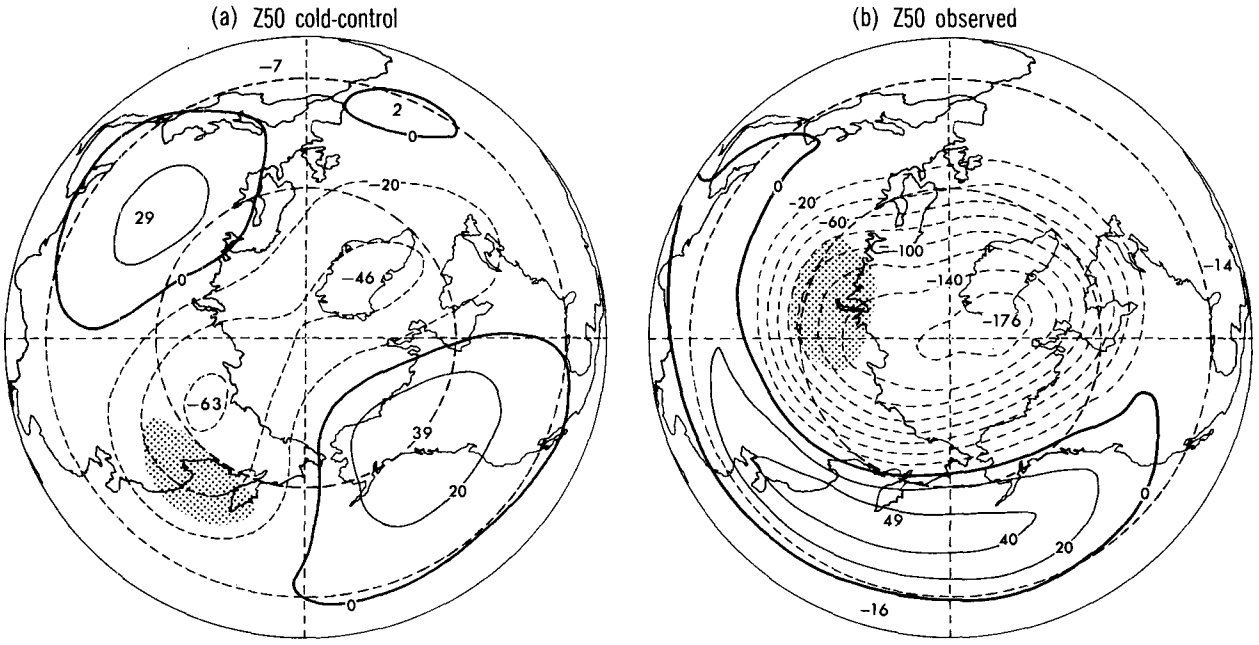

FIG. 17. As in Fig. 16 but for the 10 cold-phase experiments minus the results from the 25-year control run. The observed composite is from Hamilton (1993c).

just how extreme the confinement of the stationary waves to the tropical troposphere can be in a realistic model.

Figure 15 shows the DJF geopotential anomalies at 100 mb for the (a) warm and (b) cold perturbed experiments. At this level the anomaly in the warm perturbation case is somewhat modified from that seen lower down. In particular, the zonal structure of the anomaly is smoothed out, and the anticyclonic perturbation over Canada now dominates the cyclonic perturbation over the North Pacific. As shown below, both of these features become even more pronounced at higher levels. Some of this change with altitude can be understood as a simple consequence of the Charney–Drazin theorem (Charney and Drazin 1961), which shows that only the largest zonal wavelength stationary perturbations will propagate into the strong mean westerlies in the winter stratosphere.

Figure 16a displays the 50-mb geopotential anomaly in the warm SST perturbation integrations, while Fig. 16b shows a comparable observational result reproduced from Hamilton (1993c). In particular, Hamilton (1993c) examined DJF stratospheric geopotential data for 34 years, 9 of which he classed as at the warm extreme of the SO (i.e., at the mature phase of El Niño events), 7 as at the cold extreme, and 18 as being near normal. The result in Fig. 16b was constructed by taking the mean of the 9 warm events and subtracting the mean of the 18 normal winters. [As noted in Hamilton (1993c), these results do not change greatly if the effects of the tropical QBO (e.g., Holton and Tan 1980, 1982) are removed from the data. That could be a more appropriate comparison for the present GCM results, since the QBO is virtually absent in the SKYHI simulation.]

The tendency noted earlier for all but the zonal wave 1 and 2 components of the anomaly to be filtered out is even more pronounced at 50 mb. The model anomaly in Fig. 16a is largely a zonal wave 2 with maximum oriented roughly along the 90°W–90°E axis. There is also a wave 1 component that adds to high pressure over Canada. The observational composite has a similar character, but with the wave 1 component somewhat more prominent. The peak amplitude of the simulated anomaly is over one-third larger than that in the observed El Niño composite, presumably reflecting the large SST perturbations employed. The agreement between model and observations is actually quite impressive, considering all the dynamical links intervening between the imposed warm pool in the tropical Pacific and the planetary-scale high-latitude middle-stratospheric circulation.

Figure 17 shows the simulated mean 50-mb height anomaly compared with the observed composite anomaly for the cold SST case. Again the observations come from Hamilton (1993c). The observational results suggest that the pattern of cold phase anomalies is strongly anticorrelated with the warm phase anomalies but is considerably weaker. In fact, very little of the pattern in Fig. 17b is judged statistically significant using a local t test. The mean SKYHI anomaly in Fig. 17a is even weaker than the observed composite. It seems ap-

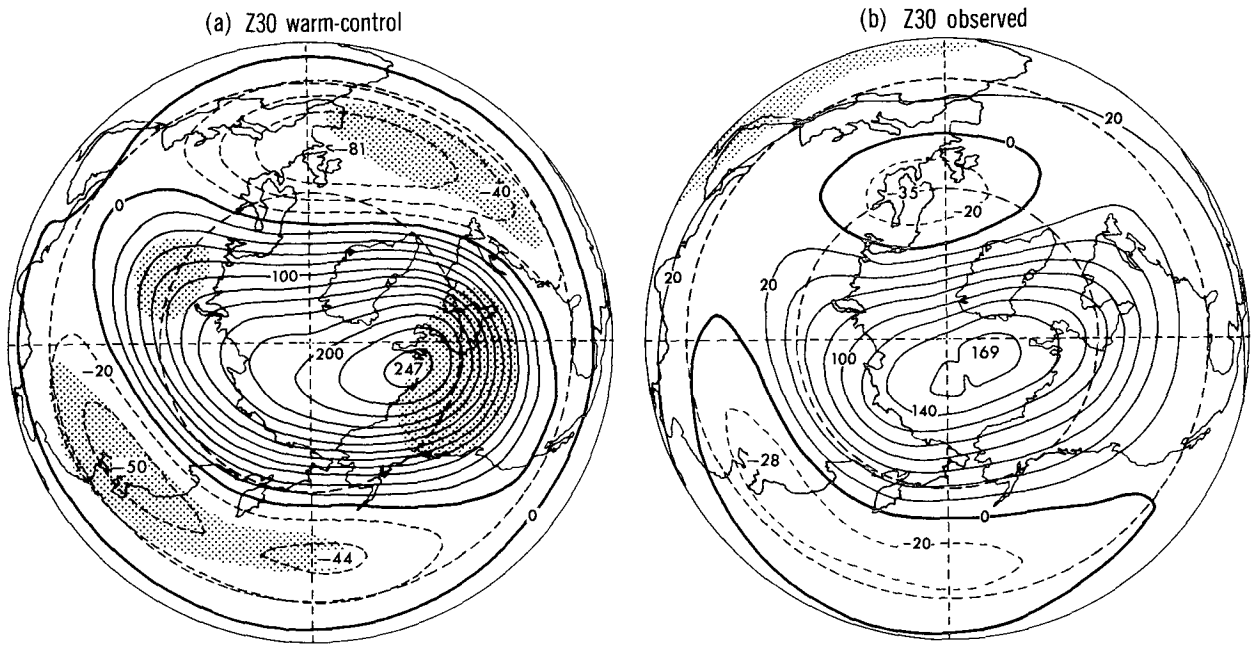

FIG. 18. As in Fig. 16 but for the 30-mb level.

parent that both longer observational records and model simulations are needed to really pin down the stratospheric effects of tropical Pacific La Niña events.

Figure 18 shows comparison of the warm-phase anomalies in model and observations at the 30-mb level. Again there is impressive agreement between the model results and observations, with the modeled anomalies being ~1.5 mb larger than observed. There is a slight westward phase tilt with height in the anomaly pattern in the stratosphere (compare Figs. 14a, 16a,

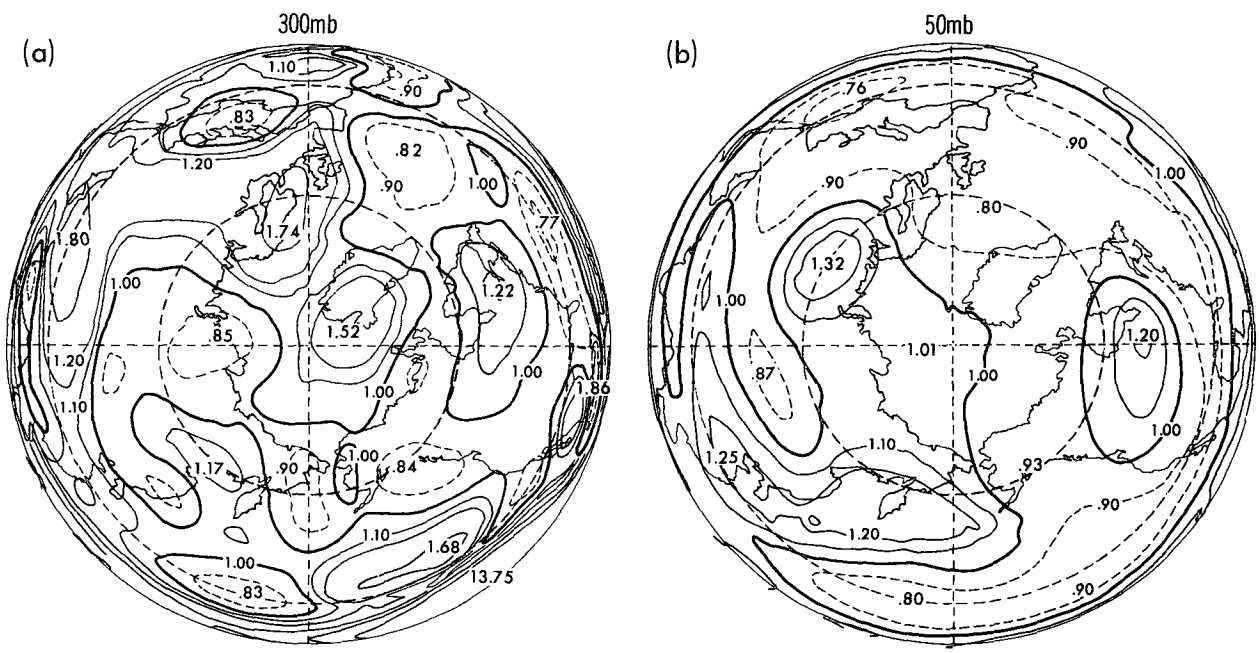

FIG. 19. The ratio of the geopotential variance in the series of 35 winters including both the control and warm SST perturbation experiments to that in the 25 control winters. Results for (a) 300 and (b) 50 mb. Contour values are 0.8, 0.9, 1.0, 1.1, 1.2, 1.6, and 2.0. Dashed contours denote regions where the ratio is less than 1.0; the 1.0 contour is heavier than the others.

and 18a). At both 50 and 30 mb the effect of the SST anomaly can be characterized roughly as a reinforcement of the mean stationary wave pattern, intensifying the Aleutian high (see Fig. 23 of HWMU). This is consistent with the tropospheric result that (again very roughly) the climatological NH stationary wave pattern is somewhat exaggerated in warm SST perturbation cases.

c. *Contribution of SST perturbations to interannual geopotential variability*

The evaluation of the interannual variability in the NH stratosphere in the control run discussed in section 3 naturally raises the question of how much of the variance in the real atmosphere is to be attributed to external causes like SST changes and how much simply results from internal atmospheric dynamics. Lau and Nath (1990; hereafter LN) addressed this issue for seasonal-mean tropospheric circulation by means of a conventional climate GCM. They performed integrations using the observed global SST evolution during the period 1960–79 and compared this with a long control integration that employed the long-term mean SST. Lau and Nath found that the interannual variability of the DJF 500-mb heights in the run with the observed SST evolution was greatly increased in the Tropics over that seen in the control integration. Their results in the extratropics are less definitive. When the geographical distribution of the ratio of the 500-mb height variance in SST and control experiments is plotted, some fairly large enhancements (~100%–200%) are found in some regions. However, LN caution that local apparent enhancements almost as large can result purely from sampling error.

The present set of experiments represents a much cruder exploration of SST effects, but the basic approach of LN can be adopted here as well. Figure 19 compares the interannual variance of DJF geopotential height in the 25 control winters versus that in a synthetic 35-year time series made up of the DJF results from the control winters and from the 10 warm perturbation experiments. Results are presented at 300 mb (Fig. 19a) and 50 mb (Fig. 19b). This comparison is quite striking, particularly in the polar cap north of ~65°N. In this region the tropospheric variance of DJF 300-mb heights is considerably enhanced (as much as 74%) in the 35-year synthetic series over that in the control run. The corresponding variance of 50-mb heights is enhanced by no more than 12% in the 35-year series, and there are actually large regions where the variance is reduced by several percent. In midlatitudes the contrast between tropospheric and stratospheric results is less strong, but is still obvious. In the Tropics the differences between tropospheric and stratospheric results are extremely large, with enormous (as much 1200% in the tropical Pacific region) enhancement of 300-mb height variability and only weak changes (~10%) in 50-mb height variability. This presumably reflects the extreme weakness of the direct penetration of the El Niño warming signal into the tropical stratosphere, noted earlier. Somewhat similar results are obtained when the variance in the control integration is compared with that in a series made up of the 25 control winters and the 10 winters from both the warm and cold perturbation experiments.

The results for the stratospheric polar cap are consistent with the following simple picture for the dynamics of that region. Even without interannual variability in the lower boundary, the GCM apparently will span some range of circulation regimes (in particular, winters with major warmings and relatively undisturbed winters will occur spontaneously). Adding the tropical Pacific SST anomalies may bias the model toward some particular pattern in a given winter (hence the average results in Figs. 16–18) but does not actually add much to the range of the model variability.

5. Experiments with imposed tropical stratospheric momentum sources

As already noted in several different contexts, an important deficiency in the SKYHI simulation is the virtual absence of a QBO in the tropical stratosphere. This is a potential concern for the simulation of extratropical variability in the model as well, since the tropical QBO is thought to influence the extratropical NH winter circulation. In particular, Holton and Tan (1980, 1982) found that at the 50-mb level the polar vortex tended to be anomalously strong (weak) during the westerly (easterly) phase of the QBO in the middle stratosphere. Baldwin and Dunkerton (1991) have shown that a similar relationship between the tropical QBO near 50 mb and the extratropical circulation apparently holds up to at least 1 mb.

There have been a number of published mechanistic model studies designed to look at the influence of the tropical QBO on extratropical stratospheric circulation. Bridger (1984), O'Sullivan and Salby (1990), Dameris and Ebel (1990), Holton and Austin (1991), and O'Sullivan and Young (1992) have all examined the effect of the tropical mean flow distribution on the model response to a prescribed pulse of stationary wave activity in midlatitudes. With the exception of Bridger (1984), all these investigators found that the presence of mean easterlies in the Tropics does promote the development of sudden warming activity in the extratropics. Kodera et al. (1991) attempted a somewhat similar study in a comprehensive GCM. In particular, they integrated their GCM through a boreal winter with prescribed easterlies in the tropical lower stratosphere and then repeated the integration with prescribed westerlies. Kodera et al. found that the time-mean vortex at different periods during the winter was not affected by the tropical winds prescribed (or even showed a slight tendency for the polar vortex to intensify in the case

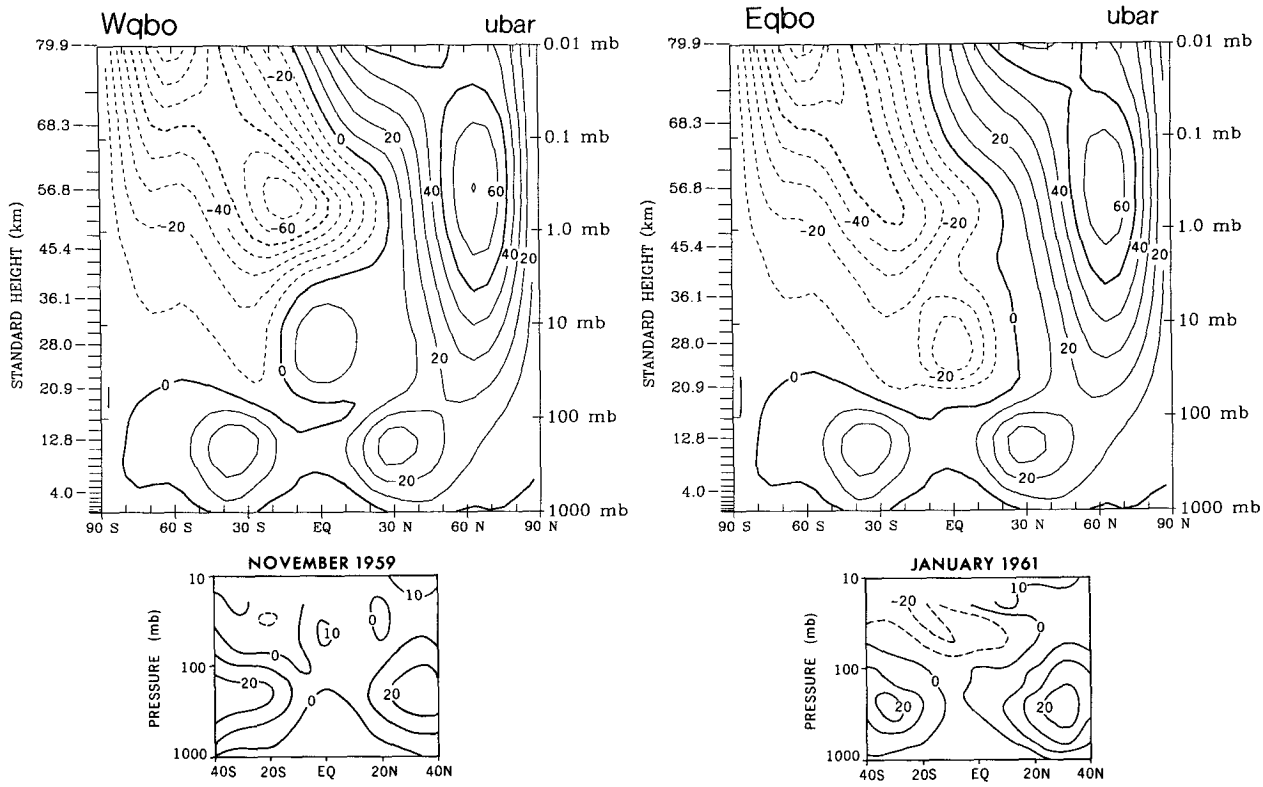

FIG. 20. Zonally averaged zonal wind cross sections. The top panels are for the December–February period averaged over the 20 westerly forced experiments (left) and over the 20 easterly forced experiments (right). The lower panels show observational results redrafted from Newell et al. (1974) for two specific months: November 1959 (left) and January 1961 (right). Note the slightly different latitude scales for the upper and lower panels. The contour interval is 10 m s^{-1}, and dashed contours denote easterly winds.

with westerly winds in the Tropics). However, rather remarkably, when they repeated their experiments after very substantially (~30%) reducing the solar constant employed, they did find the expected dependence of polar vortex strength on tropical mean winds. Interpretation of these results is difficult, however, given the small sample size and the large natural variability possible in the NH stratosphere of a comprehensive GCM.

In the present study, this issue is addressed through a series of SKYHI experiments that include arbitrary zonal-mean momentum sources imposed during the integrations to force the model tropical stratospheric winds to states similar to either the easterly or westerly QBO extremes in the real atmosphere. As in the SST experiments discussed earlier, the first series of 10 momentum source experiments ran from August through the end of February, and initial conditions were taken from 1 August of one of 10 consecutive years in the control run. The GCM code integrated was identical to the control model except that it included an arbitrary zonally symmetric source in the zonal momentum equation. This source was a relaxation to a prescribed meridional section of mean zonal wind, $\bar{u}_0(\theta, p)$. In the experiments designed to be appropriate for the westerly phase of the QBO, this $\bar{u}_0$ function took the form of an equatorially centered jet with a peak value of 21 m s^{-1} at 21.3 mb. The $\bar{u}_0$ function falls from this maximum in both height (dropping below 10 m s^{-1} on the equator at 2.82 and 49.9 mb) and latitude (Gaussian with e-folding scale of 15°). The rate of relaxation imposed also varies strongly with height and latitude. The strongest relaxation rate (0.2 day^{-1}) occurs on the equator in the middle stratosphere. The relaxation rate drops rapidly with height and latitude, so that the forcing is zero anywhere poleward of 25.5° latitude, below 103 mb, or above 1.5 mb. As a final complication, the relaxation rates were set to triple their standard values during the first month of the integration (and then restored to the standard values quoted above on 1 September). For the experiments designed to be representative of the easterly extreme of the QBO, the same form of forcing was employed except that the relaxation was to an easterly jet of twice the magnitude used for the westerly case (i.e., a peak value of u_0 of −42 m s^{-1}). This larger value was adopted since the observed maximum easterlies in the equatorial lower stratosphere are much stronger than the maximum westerlies (e.g., Wallace 1973).

After the first 10 easterly forced and 10 westerly forced 7-month integrations were completed, another

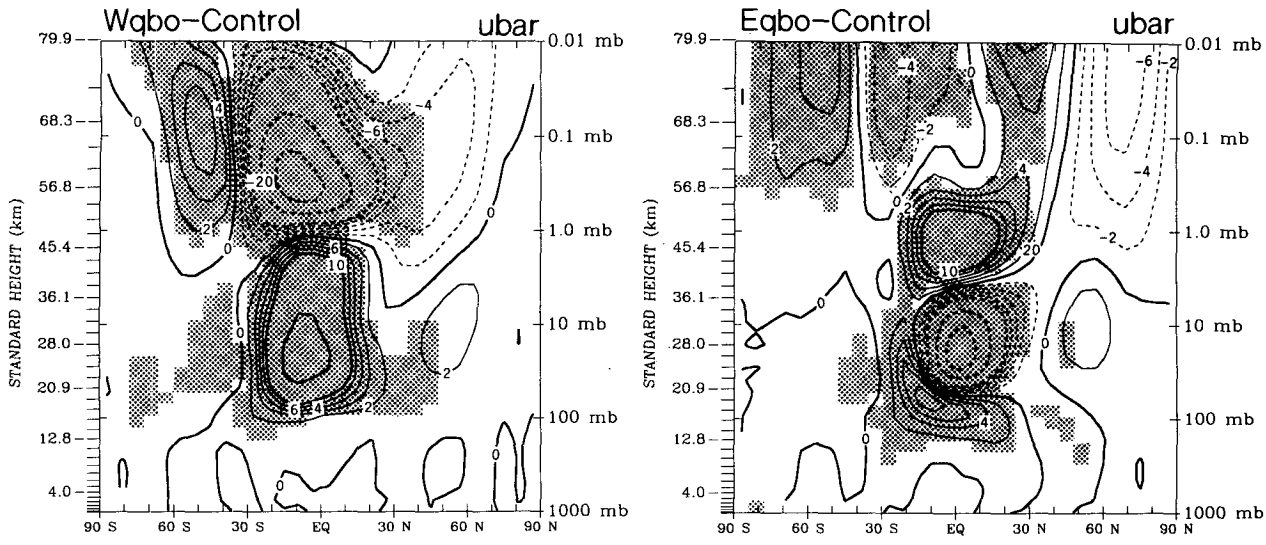

FIG. 21. The difference between the December–February mean zonal wind field in the westerly (right panel) and easterly (left panel) forced experiments and the control integration. The contour values are 0, 2, 4, 6, 8, 10, 20, and 30 m s^{-1}, and dashed contours denote negative values (i.e., winds more easterly in the forced experiments than in the control). Shading indicates regions where the results are judged significantly different from zero using a 95% criterion in a two-tailed t test.

set of 20 experiments was conducted in order to increase the number of DJF periods available for analysis. These employed exactly the same model as the other easterly and westerly forced experiments, but each extended only from October to February. The initial conditions for each of these runs were taken from the 1 October result from a corresponding 7-month integration, but with a random temperature perturbation imposed throughout the global troposphere. Other experiments have shown that the NH stratospheric flow in sets of SKYHI simulations from initial conditions perturbed in this way normally diverge within about a month. When combined with the results from the 7-month integrations, these new experiments result in a total of 40 (presumably independent) DJF periods that can be analyzed, 20 forced toward the easterly QBO extreme, and 20 forced toward the westerly QBO extreme. These are compared to a 25-year mean of the control run.

The rather ad hoc specification of the momentum source was reasonably successful in forcing realistic-looking mean flows—that is, flows that at low latitudes agreed well with observations of the extreme QBO phases and that did not have any obvious discontinuity between the circulation in the forced region and that at higher latitudes. Figure 20 shows the DJF zonal-mean zonal wind averaged over the 20 westerly forced experiments (top left) and over the 20 easterly forced experiments (top right). The bottom left panel shows the observed monthly mean wind in November 1959, as reported by Newell et al. (1974; based on their analysis of radiosonde data). This was a month in which the QBO in the lower stratosphere was near the westerly extreme. Similarly the bottom right panel shows observations for a month where the QBO was near the easterly extreme. The equatorial jets in the model results are somewhat stronger than indicated in the observations, but the zero wind line in the lower stratosphere in each case is located fairly close to where it appears in the corresponding observations.

Figure 21a shows the 20-year mean zonally averaged zonal wind in the westerly forced experiments minus that in the control run. Figure 21b shows the same quantity, but for the 20 easterly forced experiments. The most striking aspect of these figures is the production of an anomalous equatorial jet in the upper stratosphere and mesosphere of opposite sign to that forced in the lower stratosphere. This presumably results from the effects of the perturbation in the stratosphere in selectively filtering the spectrum of vertically propagating equatorial and gravity waves. The role of upward propagating waves in driving the mean flow in the SKYHI tropical middle atmosphere has been demonstrated in earlier studies (e.g., Hamilton and Mahlman 1988).

Figure 22 shows the difference between the 20-year mean DJF zonally averaged zonal wind in the easterly forced experiments and that in the 20-year mean for the westerly forced experiments. In the extratropical NH there appears to be little effect below 10 mb, while above 10 mb there is a reduction in the strength of the polar vortex in the easterly forced experiments relative to the westerly forced experiments. This reduction in vortex strength in the easterly QBO phase is in the same sense as seen in observational studies. However, the magnitude of this effect is much smaller than indicated in empirical studies. Baldwin and Dunkerton (1991) have composited the DJF mean zonal winds from Na-

tional Meteorological Center (NMC) analyses for the easterly and westerly extremes of the QBO (determined from 40-mb winds at Singapore). They find differences between their easterly and westerly composites of as much as 8 m s^{-1} near 5 mb and 60°N. This contrasts with the less than 2 m s^{-1} difference apparent at high latitudes in the present Fig. 22 at the 5-mb level. However, it should be noted that Baldwin and Dunkerton used only 12 years of data in their study. The present results are based on a total of 40 seasons. It turns out that repeating the computation of Fig. 22 using somewhat smaller samples (say 10 years in each phase) can lead to results that look much more like those of Baldwin and Dunkerton. This sampling problem is also evident in a formal analysis of statistical significance that was conducted using a t test (and assuming independence of each DJF simulation). The shading in Fig. 22 shows the regions where the difference between the easterly forced and westerly forced zonal winds were judged as 95% significant (using a two-tailed t test and assuming each winter is independent). None of the results in the NH polar vortex were found to be significant. This emphasizes the drawback of using realistic models in a sensitivity study of this kind. While the large interannual variability generated spontaneously in the control run is welcome, it does mean that long integrations may be necessary to clearly extract extratropical signals in perturbation experiments. Certainly the present results call into question studies based on a single winter of integration, such as that of Kodera et al. (1991).

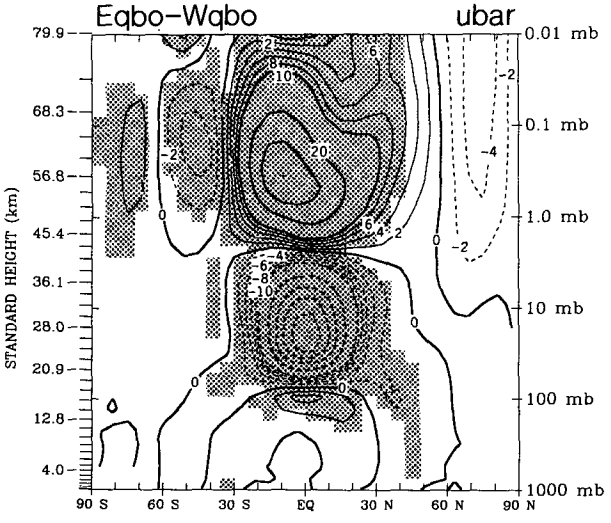

FIG. 22. The difference between the December–February mean zonally averaged zonal wind in the easterly forced experiments minus that in the westerly forced experiments. The contour values are 0, 2, 4, 6, 8, 10, 20, and 30 m s^{-1}, and dashed contours denote negative values. Shading indicates regions where the results are judged significantly different from zero using a 95% criterion in a two-tailed t test.

Interestingly, the extratropical results in Fig. 22 that are judged statistically significant are in the SH mesosphere. The magnitude of the wind difference between the two experiments is fairly small (a maximum of about 5 m s^{-1} near 65 km and 50°S), but this still stands out above the small natural interannual variability in the summer hemisphere. This midlatitude wind anomaly might be caused by the effects of the diabatic circulation induced by the large tropical forcing in the upper stratosphere and mesosphere, or it could reflect the tropical mean flow filtering of gravity waves generated in the tropical lower atmosphere and propagating into the extratropical mesosphere. The work of Manzini and Hamilton (1993) has demonstrated that a significant fraction of the extratropical mesospheric gravity waves in the SKYHI model are forced by convection in the low-latitude troposphere. The SH result in Fig. 22 is interesting in light of the limited rocket observations that suggest an extratropical mesospheric extension of the familiar tropical stratospheric QBO (Groves 1973).

6. Equilibration of the stratospheric water vapor field

This section presents a brief examination of the long-term equilibration of the water vapor distribution in the SKYHI model stratosphere. This is admittedly somewhat tangential to the main purpose of this paper, but the availability of the very long N30 integration represents an unprecedented opportunity to examine this issue in a 3D GCM with a serious representation of the middle atmosphere. The importance of the timescale of equilibration for coupled dynamical–photochemical models is evident, and attempts have been made to determine similar timescales from observations and from simple models. For example, Garcia and Solomon (1983) estimate a residence time of roughly 1 year for the lower stratosphere in their 2D photochemical–transport model. Holton (1990) used an indirect observational determination of the transport across the 100-mb surface to infer a turnover time of 2.5 years for the atmospheric layer lying above 100 mb.

It should be noted that the equilibrium water vapor distribution in the model stratosphere is expected to be somewhat unrealistic. The lack of the well-known in situ chemical source (oxidation of methane) and the unrealistically cold tropopause temperature (and hence an overly desiccated source of tropospheric air) are certain to result in unrealistically low simulated stratospheric mixing ratios. However, assuming that the transport processes are reasonably well represented in the model, these other deficiencies should not appreciably affect the equilibration timescale. The drop in stratospheric mixing ratios from the initially specified values in the model is actually a nice indication of the model stratosphere filling up with tropospheric air that has passed through the tropopause "cold trap." The

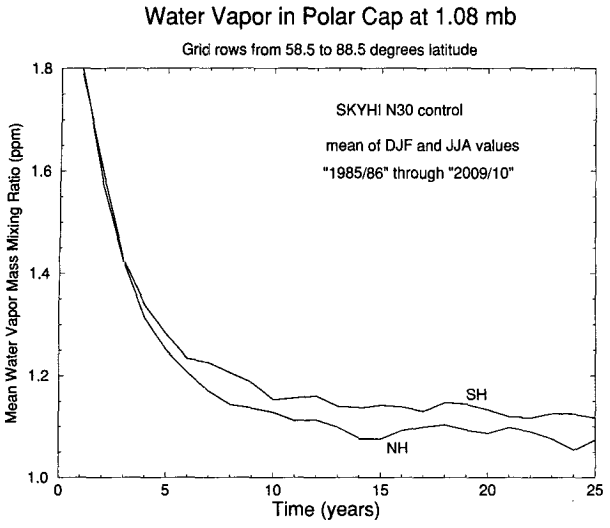

FIG. 23. The time evolution of the water vapor mass mixing ratio averaged over polar cap regions at 1.08 mb through the N30 control integration. Each yearly value represents a mean of a JJA and a DJF average. Year 1 represents JJA *1985* and DJF *1985/86,* and so on. The average is an area-weighted mean over all the grid rows poleward of 58° latitude. Results presented separately for the Northern Hemisphere (NH) and Southern Hemisphere (SH) polar caps.

time for this tropospheric air to replace the stratospheric inventory is likely a crucial timescale for stratospheric equilibration of any long-lived tracer with a tropospheric source or sink.

Figure 23 shows the average water vapor mass mixing ratios for the polar caps at 1.08 mb for each of 25 consecutive years of the control N30 integration. Results for the Tropics (not shown) are very similar. By *1985* when the detailed N30 data were first archived (and Fig. 23 begins) the 1.08-mb mixing ratios had dropped to about 1.8 ppmm (from the 2.5 ppmm specified in the original *1978* initialization; see HWMU). The mixing ratios continue to drop noticeably for the next decade or so and then appear to equilibrate at about 1.12 (SH) and 1.08 (NH) ppmm. The approach to equilibrium is roughly exponential with an e-folding timescale of just under 4 years. This compares reasonably well with Holton's estimate of 2.5 years [the lifetime for upper-stratospheric air is likely to be longer than for the entire atmospheric layer considered by Holton; see Mahlman and Moxim (1978)]. The results reaffirm that comprehensive dynamical–photochemical models must be run for rather substantial periods in order to guarantee equilibration of the chemical constituents.

Just as for many other aspects of the model results described in this paper, much more analysis could be performed on the stratospheric water vapor budget. For example, the cause of the interhemispheric gradient in the equilibrated water vapor field evident in Fig. 23 could be determined. It would also be interesting to apply Holton's (1990) technique to the model data and to then compare the results with the present direct determination of the stratospheric residence time.

7. Conclusions

This paper has reported on an investigation of day-to-day and interannual variability in the NH stratospheric circulation as simulated in a sophisticated, troposphere–stratosphere–mesosphere GCM. In a companion paper (HWMU) the basic NH winter stratospheric simulation was shown to be in reasonably good agreement with observations. In particular, the problem of an unrealistically intense polar vortex that plagued earlier simulations is largely eliminated. One expects the mean strength of the vortex and the degree of interannual variability to be closely related, since a strong vortex is less penetrable by quasi-stationary waves (Charney and Drazin 1961; McIntyre 1982). It is heartening that the good SKYHI NH mean polar vortex simulation is accompanied by a realistic degree of interannual variability. By contrast, the simulated SH vortex is known to be unrealistically strong (HWMU), and the interannual variability is also weaker than observed (Mahlman et al. 1994).

One apparent bias in the control simulation is the tendency for major warmings to occur too frequently in December (and thus for the model to overestimate the interannual temperature variance in December, at least above 10 mb). It is worthwhile to consider whether this may be related to deficiencies in the mean simulation as well. It has been noted that observed sudden warmings often have two stages. Many very strong warmings are preceded by a smaller wave event that apparently causes erosion of the edge of the high potential vorticity core to "precondition" the vortex to be penetrated by a later wave pulse (McIntyre 1982). The SKYHI model seems to have a tendency for the vortex to be somewhat too strongly confined near the pole, particularly in the upper stratosphere (HWMU). This unrealistically small vortex may thus be in what might be termed a permanently preconditioned state. Thus, it may be more subject than the polar vortex in the real atmosphere to breakdown by the first significant wave pulse of the winter.

While the focus of this paper has been on the winter in the extratropical NH, it was noted that the SKYHI model also does not reproduce the degree of interannual temperature variability in the tropical and summer hemisphere middle atmosphere that is apparent in the NMC analyses. Part of this problem lies in the virtual absence of the QBO in the model (the QBO in temperature in the real atmosphere has a peak amplitude ~2°C), but it is also conceivable that the variability is overestimated in the observations. Certainly it is easy to imagine effects (such as the spurious inhomogeneities in the observational record or changes in atmospheric composition) that could add ~1°C to the interannual variance estimated from several years of NMC data.

A series of simple tropical SST perturbation experiments was conducted to estimate the effects on the SKYHI simulated stratosphere. The observed influence of the SO on the extratropical winter stratospheric circulation was well reproduced in these experiments. It was demonstrated that the direct penetration of the effects of the SST anomalies into the tropical stratosphere is extremely weak in the model. This suggests that little connection will be found between the tropospheric SO and any aspect of the circulation in the tropical stratosphere.

Just as in the companion paper (HWMU), the approach in the present paper has been somewhat descriptive. There are many aspects of both the control and perturbation simulations that require further analysis and investigation. To conclude this paper, a few proposed projects along these lines will be mentioned. First, the detailed dynamics of the sudden warmings as well as the implications of the model results for the predictability of stratospheric warmings are now being studied through additional detailed analysis and new model experiments. The SKYHI control integration itself is being continued with the intention of confirming the peculiar decadal variability seen in polar temperatures. This issue might also be addressed by means of long integrations with a simplified model. These would be similar to those already reported by James and James (1992) but should also include a radiative forcing that can produce a reasonable stratosphere, a forcing mechanism for stationary waves, and a seasonal cycle. Finally, the impressive SKYHI simulation of the observed El Niño effects in the extratropical stratosphere represents a very challenging case for the application of simplified models of stationary waves. Such models have had some success in explaining the tropospheric response of GCMs to imposed tropical SST anomalies (e.g., Ting and Held 1990). It would be interesting to see how well such models can handle the propagation of the extratropical stationary wave anomaly into the winter stratosphere (with its large time-mean zonal asymmetries).

Acknowledgments. The author wishes to thank R. J. Wilson for his assistance in setting up the control integration and J. D. Mahlman for helpful discussions. Y. Hayashi, N.-C. Lau, J. D. Mahlman, E. Manzini, and R. J. Wilson provided helpful comments on the manuscript. B. Naujokat and H. van Loon kindly allowed permission to reproduce previously published figures.

REFERENCES

Andrews, D. G., J. R. Holton, and C. B. Leovy, 1987: *Middle Atmosphere Dynamics.* Academic Press, 489 pp.

Austin, J., N. Butchart, and K. P. Shine, 1992: Possibility of an Arctic ozone hole in a doubled-CO_2 climate. *Nature,* **360,** 221–225.

Baldwin, M. P., and T. J. Dunkerton, 1991: Quasi-biennial oscillation above 10 mb. *Geophys. Res. Lett.,* **18,** 1205–1208.

Barnett, T. P., 1991: The interaction of multiple timescales in the tropical climate system. *J. Climate,* **4,** 269–285.

Boer, J. G., 1985: Modelling the atmospheric response to the 1982/83 El Niño. *Coupled Ocean–Atmosphere Models,* C. J. C. Nihoul, Ed., Elsevier, 7–17.

Boville, B. A., 1986: Wave–mean flow interactions in a general circulation model of the troposphere and stratosphere. *J. Atmos. Sci.,* **43,** 1711–1725.

——, 1991: Sensitivity of the simulated climate to model resolution. *J. Climate,* **4,** 469–485.

Bridger, A. F. C., 1984: A numerical test of connections between the stratospheric sudden warmings and the quasi-biennial oscillation. *J. Geophys. Res.,* **89,** 4826–4832.

Brier, G. W., 1978: The quasi-biennial oscillation and feedback processes in the atmosphere–ocean–earth system. *Mon. Wea. Rev.,* **106,** 938–946.

Cariolle, D., M. Amodei, M. Deque, J.-F. Mahfouf, P. Simon, and H. Teyssedre, 1993: A quasi-biennial oscillation signal in general circulation model simulations. *Science,* **261,** 1313–1316.

Charney, J. G., and P. G. Drazin, 1961: Propagation of planetary-scale disturbances from the lower into the upper atmosphere. *J. Geophys. Res.,* **66,** 83–109.

Dameris, M., and A. Ebel, 1990: The quasi-biennial oscillation and major stratospheric warmings: A three-dimensional model study. *Ann. Geophys.,* **8,** 79–86.

Garcia, R. R., and S. Solomon, 1983: A numerical model of the zonally averaged dynamical and chemical structure of the middle atmosphere. *J. Geophys. Res.,* **88,** 1379–1400.

Groves, G. V., 1973: Zonal wind quasi-biennial oscillations at 25–60 km altitude, 1962–1969. *Quart. J. Roy. Meteor. Soc.,* **99,** 73–81.

Hamilton, K., 1988: A detailed examination of the extratropical effects of El Niño/Southern Oscillation events. *J. Climatol.,* **8,** 67–86.

——, 1993a: What we can learn from general circulation models about the spectrum of middle atmospheric motions. *Coupling Processes in the Lower and Middle Atmosphere,* E. Thrane, T. Blix, and D. Fritts, Eds., Kluwer Academic, 161–174.

——, 1993b: A general circulation model simulation of El Niño effects in the extratropical Northern Hemisphere stratosphere. *Geophys. Res. Lett.,* **20,** 1803–1806.

——, 1993c: An examination of observed Southern Oscillation effects in the Northern Hemisphere stratosphere. *J. Atmos. Sci.,* **50,** 3468–3473.

——, 1994: Modelling middle atmosphere interannual variability. *Fifth COSPAR Colloq.,* M. Teague, Ed., Pergamon Press, 751–757.

——, and J. D. Mahlman, 1988: General circulation model simulation of the semiannual oscillation in the tropical middle atmosphere. *J. Atmos. Sci.,* **44,** 3212–3235.

——, and L. Yuan, 1992: Experiments on tropical stratospheric mean wind variations in a spectral general circulation model. *J. Atmos. Sci.,* **49,** 2464–2483.

——, R. J. Wilson, J. D. Mahlman, and L. J. Umscheid, 1995: Climatology of the GFDL SKYHI troposphere–stratosphere–mesosphere general circulation model. *J. Atmos. Sci.,* **52,** 5–43.

Holton, J. R., 1990: On the global exchange of mass between the stratosphere and troposphere. *J. Atmos. Sci.,* **47,** 392–395.

——, and H.-C. Tan, 1980: The influence of the equatorial quasi-biennial oscillation on the global circulation at 50 mb. *J. Atmos. Sci.,* **40,** 1410–1425.

——, and ——, 1982: The quasi-biennial oscillation in the Northern Hemisphere lower stratosphere. *J. Meteor. Soc. Japan,* **60,** 140–147.

——, and J. Austin, 1991: The influence of the QBO on sudden stratospheric warmings. *J. Atmos. Sci.,* **48,** 607–618.

James, I. N., and P. M. James, 1992: Spatial structure of ultra-low frequency variability of the flow in a simple atmospheric circulation model. *Quart. J. Roy. Meteor. Soc.,* **118,** 1211–1233.

Kodera, K., M. Chiba, and K. Shibata, 1991: A general circulation model study of the solar and QBO modulation of the stratospheric circulation during Northern Hemisphere winter. *Geophys. Res. Lett.,* **18,** 1209–1212.

Labitzke, K., 1987: Sunspots, the QBO, and stratospheric temperature in the North Polar Region. *Geophys. Res. Lett.*, **14,** 535–537.

Lau, N.-C., and M. J. Nath, 1990: A general circulation model study of the atmospheric response to extratropical SST anomalies observed in 1960–79. *J. Climate,* **3,** 965–989.

Leovy, C. B., C.-R. Sun, M. H. Hitchmann, E. E. Remsberg, J. M. Russell III, L. L. Gordley, J. C. Gille, and L. V. Lyjak, 1985: Transport of ozone in the middle stratosphere: Evidence for planetary wave breaking. *J. Atmos. Sci.,* **42,** 230–244.

Mahlman, J. D., and W. J. Moxim, 1978: Tracer simulation using a global general circulation model: Results from a midlatitude instantaneous source experiment. *J. Atmos. Sci.,* **35,** 1340–1374.

——, and L. J. Umscheid, 1987: Comprehensive modeling of the middle atmosphere: The influence of horizontal resolution. *Transport Processes in the Middle Atmosphere,* G. Visconti and R. Garcia, Eds., D. Reidel, 251–266.

——, J. P. Pinto, and L. J. Umscheid, 1994: Transport, radiative, and dynamical effects of the Antarctic ozone hole: A GFDL "SKYHI" model experiment. *J. Atmos. Sci.,* **51,** 489–508.

Manabe, S., and J. D. Mahlman, 1976: Simulation of seasonal and interhemispheric variations in the stratospheric circulation. *J. Atmos. Sci.,* **33,** 2185–2217.

Manzini, E., and K. Hamilton, 1993: Middle atmospheric traveling waves forced by latent and convective heating. *J. Atmos. Sci.,* **50,** 2180–2200.

McIntyre, M. E., 1982: How well do we understand the dynamics of stratospheric warmings? *J. Meteor. Soc. Japan,* **60,** 37–65.

Naujokat, B., K. Labitzke, R. Lenschow, K. Petzoldt, and R.-C. Wohlfart, 1988: The stratospheric winter 1987/88: An unusually early major midwinter warming. *Beilage zur Berliner Wetterakarte,* No. 6, 20 pp.

Newell, R. E., J. W. Kidson, D. G. Vincent, and G. J. Boer, 1974: *The General Circulation of the Tropical Atmosphere and Interactions with Extratropical Latitudes.* The MIT Press.

O'Sullivan, D., and M. L. Salby, 1990: Coupling of the quasi-biennial oscillation and the extratropical circulation in the stratosphere through planetary wave transport. *J. Atmos. Sci.,* **47,** 650–673.

——, and R. E. Young, 1992: Modeling the quasi-biennial oscillation's effect on the winter stratospheric circulation. *J. Atmos. Sci.,* **49,** 2437–2448.

Pan, Y.-H., and A. H. Oort, 1983: Global climate variations connected with sea surface temperature anomalies in the eastern equatorial Pacific Ocean for the 1958–73 period. *Mon. Wea. Rev.,* **111,** 1244–1258.

Philander, S. G. H., 1990: *El Niño, La Niña and the Southern Oscillation.* Academic Press, 289 pp.

Randel, W. J., 1992: Global atmospheric circulation statistics, 1000-1 mb. NCAR Tech. Note TN-366+STR, 256 pp.

Rasmusson, E. M., and T. Carpenter, 1982: Variations in tropical sea surface temperature and surface wind fields associated with the Southern Oscillation/El Niño. *Mon. Wea. Rev.,* **110,** 354–384.

Rind, D., R. Suozzo, N. K. Balachandran, A. Lacis, and G. Russell, 1988a: The GISS global climate–middle atmosphere model. Part I: Model structure and climatology. *J. Atmos. Sci.,* **45,** 329–370.

——, ——, and ——, 1988b: The GISS global climate–middle atmosphere model. Part II: Model variability due to interactions between planetary waves, the mean circulation and gravity wave drag. *J. Atmos. Sci.,* **45,** 371–386.

Strahan, S. E., and J. D. Mahlman, 1994a: Evaluation of the GFDL "SKYHI" general circulation model using aircraft N_2O measurements: 1. Polar winter stratospheric meteorology and tracer morphology. *J. Geophys. Res.,* **99,** 10 305–10 318.

——, and ——, 1994b: Evaluation of the GFDL "SKYHI" general circulation model using aircraft N_2O measurements: 2. Tracer variability and diabatic meridional circulation. *J. Geophys. Res.,* **99,** 10 319–10 332.

Ting, M., and I. M. Held, 1990: The stationary wave response to a tropical SST anomaly in an idealized GCM. *J. Atmos. Sci.,* **47,** 2546–2566.

van Loon, H., and R. A. Madden, 1981: The Southern Oscillation. Part I: Global associations with pressure and temperature in northern winter. *Mon. Wea. Rev.,* **109,** 1150–1162.

——, and D. J. Shea, 1985: The Southern Oscillation. Part IV: The precursors south of 15°S to the extremes of the oscillation. *Mon. Wea. Rev.,* **113,** 2063–2074.

——, and K. Labitzke, 1987: The Southern Oscillation. Part V: The anomalies in the lower stratosphere of the Northern Hemisphere in winter and a comparison with the quasi-biennial oscillation. *Mon. Wea. Rev.,* **115,** 357–369.

——, R. L. Jenne, and K. Labitzke, 1972: Climatology of the stratosphere in the Northern Hemisphere. *Meteor. Abhand.,* **100,** No. 5, 162 pp.

Wallace, J. M., 1973: General circulation of the tropical lower stratosphere. *Rev. Geophys. Space Phys.,* **11,** 191–222.